



Published in final edited form as:

*Synapse*. 2021 October ; 75(10): e22218. doi:10.1002/syn.22218.

## Acute Delta 9-tetrahydrocannabinol administration differentially alters the hippocampal opioid system in adult female and male rats

Kyle A. Windisch<sup>#1</sup>, Sanoara Mazid<sup>#2</sup>, Megan A. Johnson<sup>2</sup>, Elina Ashirova<sup>2</sup>, Yan Zhou<sup>1</sup>, Lennox Gergoire<sup>2</sup>, Sydney Warwick<sup>2</sup>, Bruce S McEwen<sup>3,\*+</sup>, Mary Jeanne Kreek<sup>1,\*++</sup>, Teresa A. Milner<sup>1,2,\*</sup>

<sup>1</sup>The Laboratory of the Biology of Addictive Diseases, The Rockefeller University, 1230 York Avenue, New York, NY 10065

<sup>2</sup>Feil Family Brain and Mind Research Institute, Weill Cornell Medicine, 407 East 61st Street, New York, NY 10065

<sup>3</sup>Harold and Margaret Milliken Hatch Laboratory of Neuroendocrinology, The Rockefeller University, 1230 York Avenue, New York, NY 10065

# These authors contributed equally to this work.

### Abstract

Our prior studies demonstrated that the rat hippocampal opioid system can undergo sex-specific adaptations to external stimuli that can influence opioid-associated learning processes. This opioid system extensively overlaps with the cannabinoid system. Moreover, acute administration of <sup>9</sup>Tetrahydrocannabinoid (THC), the primary psychoactive constituent of cannabis, can alter cognitive behaviors that involve the hippocampus. Here we use light and electron microscopic immunocytochemical methods to examine the effects of acute THC (5 mg/kg, i.p. 1 hour) on mossy fiber Leu-Enkephalin (LEnk) levels and the distribution and phosphorylation levels of delta and mu opioid receptors (DORs and MORs, respectively) in CA3 pyramidal cells and parvalbumin dentate hilar interneurons of adult female and male Sprague-Dawley rats. In females with elevated estrogen states (proestrus/estrus stage), acute THC altered the opioid system so that it resembled that seen in vehicle-injected females with low estrogen states (diestrus) and males: 1) mossy fiber LEнк levels in CA2/3a decreased; 2) phosphorylated-DOR levels in CA2/3a pyramidal cells increased; and 3) phosphorylated-MOR levels increased in most CA3b laminae. In males, acute THC resulted in the internalization of MORs in parvalbumin-containing interneuron dendrites

---

Corresponding author: Dr. Kyle Windisch, The Laboratory of the Biology of Addictive Diseases, The Rockefeller University, 1230 York Avenue, New York, NY 10065 United States of America, Phone: (212) 327-8490, FAX: (212) 327-8574, [kwindisch01@rockefeller.edu](mailto:kwindisch01@rockefeller.edu); [tmilner@med.cornell.edu](mailto:tmilner@med.cornell.edu).

\*Co-Senior Investigators

<sup>+</sup>Deceased January 2, 2020

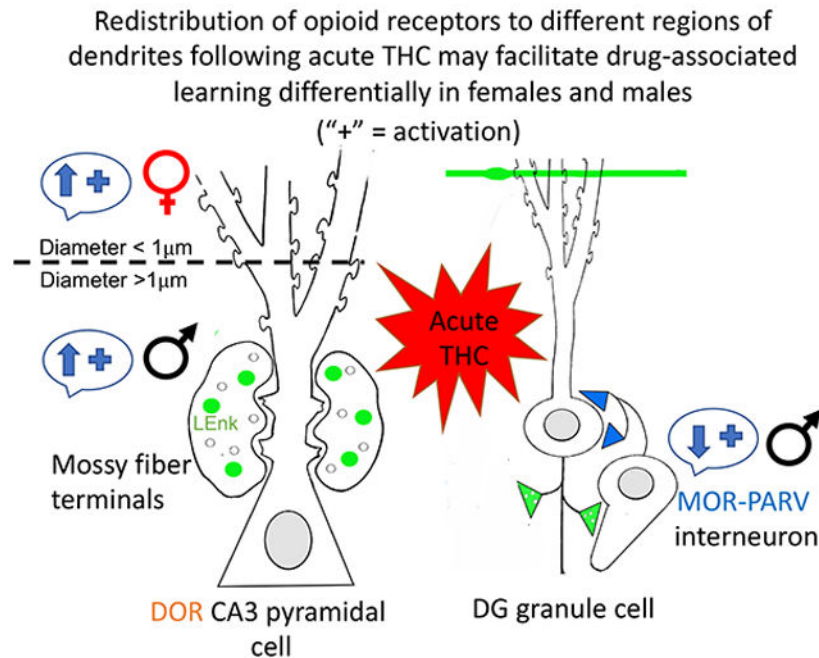
<sup>++</sup>Deceased March 27, 2021

**Author Contributions:** T.A.M., M.J.K. and B.S.M. designed research and obtained funding; K.A.W, S.M., M.A.J., E.A., Y.Z, L.G., S.W. and T.A.M. performed research; K.A.W, S.M., L.G., S.W. and T.A.M. analyzed data; K.A.W., S.M., T.A.M., B.S.M.\*, M.J.K.\* wrote the paper. \*B.S.M. and M.J.K. contributed to abstract and poster presented at American College of Neuropsychopharmacology (ACNP) meeting 2019.

**Conflict of Interest:** The authors declare no competing financial interests.

which would decrease disinhibition of granule cells. In both sexes, acute THC redistributed DORs to the near plasma membrane of CA3 pyramidal cell dendrites, however, the dendritic region varied with sex. Additionally, acute THC also resulted in a sex-specific redistribution of DORs within CA3 pyramidal cell dendrites which could differentially promote synaptic plasticity and/or opioid-associated learning processes in both females and males.

## Graphical Abstract



## Keywords

sex differences; 9-tetrahydrocannabinol; delta opioid receptor; hippocampal CA3

## INTRODUCTION

With the rise in prescription opioid use and abuse (Centers for Disease Control and Prevention, 2019), it is imperative to elucidate the factors that alter the susceptibility to opioid addiction. Addictive mechanisms require associative memory and motivational incentives (Koob and Volkow, 2010) that critically involve hippocampal output relayed directly or indirectly to the mesolimbic reward system (Vorel et al., 2001; Luo et al., 2011). Intrinsic hippocampal circuitry supports spatial and episodic memory acquisition processes essential for associating a drug of abuse with a particular place and set of events (Koob and Volkow, 2010, 2016). In particular, opioid signaling in the CA3 region has been shown to play a critical role in spatial memory and in contextual associative learning (Meilandt et al., 2004; Kesner and Warthen, 2010).

Our prior studies in Sprague-Dawley rats have demonstrated that the hippocampal opioid system can undergo sex-specific adaptations to the hormonal milieu and external stimuli that

can influence these opioid-associated learning processes. In brief, females in high estrogen states (proestrus), but not in low estrogen states (diestrus) nor in males, exhibit a form of opioid-mediated long-term potentiation (LTP) in mossy fiber - CA3 pyramidal cell synapses (Harte-Hargrove et al., 2015). Females with elevated estrogen states (proestrus/estrus) also have: 1) elevated Leu-Enkephalin (LEnk) levels in mossy fibers (Torres-Reveron et al., 2008; Pierce et al., 2014), 2) increased delta opioid receptors (DORs) in CA3 pyramidal cell spines contacted by mossy fibers (i.e., MF-CA3 synapses) (Harte-Hargrove et al., 2015; Mazid et al., 2016); and 3) increased plasma membrane mu opioid receptors (MORs) on parvalbumin (PARV)-containing hilar interneurons (Torres-Reveron et al., 2009; Milner et al., 2013). Following oxycodone conditioned place preference (CPP), estrus females exhibit an additional increase in near-plasmalemmal DORs in GABAergic interneuron dendrites known to contain neuropeptide Y (Ryan et al., 2018) as well as elevated phosphorylated MOR (pMOR) levels in CA1 and CA3a,b (Bellamy et al., 2019). In males, oxycodone CPP redistributes DORs to MF CA3 synapses (Ryan et al., 2018) and elevates phosphorylated DOR (pDOR) levels in pyramidal cell dendrites in CA2/3a (Bellamy et al., 2019). Oxycodone CPP also induces sex-specific changes in plasticity, stress and kinase markers in these same hippocampus circuits (Randesi et al., 2019). Thus, elevated estrogen levels and oxycodone CPP induce sex-specific changes in the hippocampal opioid system that would enhance opioid-mediated learning processes.

Chronic immobilization stress (CIS) also differentially affects the hippocampal opioid system in female and male rats which can have important functional implications. CIS elevates mossy fiber LEnk levels and redistributes DORs and MORs in hippocampal neurons so that all females, regardless of estrogen state, are “primed” for learning processes (Mazid et al., 2016; McEwen and Milner, 2017). In contrast, CIS in males, but not females, results in dendritic retraction of DOR-containing CA3 pyramidal cells and a loss of MOR-containing PARV interneuron (McEwen and Milner, 2017). Moreover, CIS in males “shuts down” the trafficking and activation of DORs and MORs in hippocampal neurons (Mazid et al., 2016; McEwen and Milner, 2017; Bellamy et al., 2019). These changes in CIS males also are accompanied by a down-regulation in the expression of several plasticity genes and proteins (Randesi et al., 2018). Additionally, our recent studies have shown that CIS “resets” baseline sex differences in opioid gene expression in a manner that would promote opioid mediated learning in females, but not males (Johnson et al., 2020). The sex-specific changes in the hippocampal opioid system likely impact network properties and synaptic plasticity processes that contribute to the attenuation of oxycodone CPP in CIS males (Bellamy et al., 2019; Reich et al., 2019).

Several lines of evidence indicate that cannabinoids can also influence opioid associative learning processes. Anatomically, the opioid and cannabinoid systems extensively overlap in the hippocampus. Cannabinoid receptors type 1 (CB1) are densely expressed on GABAergic interneuron terminals (Nyiri et al., 2005). Many CB1 terminals arise from cholecystokinin (CCK) containing interneurons (Marsicano and Lutz, 1999; Tsou et al., 1999), which are known to synapse on PARV-containing interneurons to affect their network properties (Karson et al., 2009). CB1s also are in terminals that synapse on DOR-containing pyramidal cells and regulate cannabinoid-dependent suppression of excitatory transmission (Kawamura et al., 2006). In female CB1 knockout mice, mossy fiber LEnk levels and the number of

hilar neuropeptide Y (NPY) neurons (which contain DORs) are reduced (Rogers et al., 2016). Type 2 cannabinoid receptors (CB2) are highly expressed in pyramidal cell bodies and dendrites (Brusco et al., 2008a; Brusco et al., 2008b). Fatty acid amide hydrolase, which metabolizes endocannabinoids, is found in the pyramidal and granule cell soma and dendrites but not interneurons (Gulyas et al., 2004; Morozov et al., 2004). Monoglyceride lipase, a key enzyme in the hydrolysis of 2-arachidinoyl glycerol, is contained in granule cell mossy fibers, CA3 pyramidal cells and some interneurons (Gulyas et al., 2004). In adult male rats, pre-exposure to CB1 agonists strengthens morphine CPP (Manzanedo et al., 2004) and both CB1 agonist and <sup>9</sup>Tetrahydrocannabinoid (THC), the primary psychoactive constituent of cannabis (Mechoulam and Parker, 2013), can increase heroin self-administration (Solinas et al., 2005).

Recent studies in the CA1 region of male mice have demonstrated that acute THC can increase the percentage of CB1 terminals forming symmetric synapses and increase the area of pyramidal cell dendrites but decrease the size of dendritic spines (Bonilla-Del Río et al., 2020). However, it is unknown whether acute THC induces changes in the hippocampal opioid system and whether these changes are sex-specific. Thus, in the present study we used light and electron microscopic immunocytochemical methods to examine the effects acute THC administration on the hippocampal opioid system in female and male rats.

## MATERIALS AND METHODS

### Animals

Experimental procedures were approved by the Institutional Animal Care and Use Committee of The Rockefeller University and Weill Cornell Medicine and were in accordance with the 2011 Eighth Edition of the National Institute of Health Guide for the Care and Use of Laboratory Animals. A single cohort of 24 male and female Sprague-Dawley rats (10 weeks old at the time of shipping) obtained from Charles River Laboratories (Wilmington, MA) were used. Rats from each sex were housed 2-3 per cage with *ad libitum* access to food and water on a standard 12h:12h light cycle (lights on at 7am). To minimize stress, the rats were allowed to acclimate to the vivarium for 1 week and gently handled by the same experimenter for 5 days prior to the experiment to reduce stress levels (Deutsch-Feldman et al., 2015).

### THC injection

(-)-THC in 95% ethanol was obtained from the National Institute on Drug Abuse Drug Supply System (catalogue #7370-001). A final concentration of 5 mg/ml THC in 7.75% Tween80 in saline (vehicle; VEH) was prepared as described by Pickel et al (Pickel et al., 2020). A dose of 5 mg/kg [corresponding to an estimated human equivalent of 0.8 mg/kg or roughly 49 mg THC for a human (Nair and Jacob, 2016)], was selected as it produces roughly equivalent peak plasma THC concentrations and total drug exposure in male and female rats as those observed in humans following voluntary cannabis inhalation (Huestis et al., 1992; Cooper and Haney, 2009; Ruiz et al., 2020). This moderate dose has been used by others in mice and rats to study acute effects of THC (de Miguel et al., 1998; Hernández-Tristán et al., 2000; Bonilla-Del Río et al., 2020; Ruiz et al., 2020). Female and

male rats were separated randomly into experimental groups. Rats received either a single dose of 5 mg/kg THC (i.p.) or VEH (controls) and returned to their home-cage for 1 hour prior to euthanasia.

### Estrus cycling determination

Estrus cycling was performed using vaginal smear cytology (Turner and Bagnara, 1971) following anesthesia on the day of euthanasia. Estrus phases were characterized as either proestrus (elevated estrogen levels), estrus (declining estrogen levels and elevated progesterone levels) and diestrus (low estrogen and progesterone levels). On the day of euthanasia, all THC-injected females were in proestrus/estrus whereas 3 of 6 VEH injected females were in proestrus/estrus.

### Tissue Preparation

Brain tissue was prepared as previously described (Milner et al., 2011). Briefly, rats were deeply anesthetized with a Ketamine (100mg/kg) /Xylazine (10 mg/kg) cocktail (i.p.) and fixed by aortic arch perfusion sequentially with: 1) 10-15 ml saline (0.9%) containing 2% heparin; 2) 50 ml of 3.75% acrolein (Polysciences, Washington, PA) and 2% paraformaldehyde [PFA; Electron Microscopy Sciences (EMS) Hatfield, PA] in 0.1 M phosphate buffer (PB; pH 7.4), and 3) 200 ml of 2% PFA in PB. Brains were extracted from the skull, cut into a 5 mm thick coronal block using a brain matrix (ASI Instruments Inc., Warren, MI) and postfixed for 1 hour in 2% PFA in PB. Brains then were coronally sectioned (40  $\mu$ m thick) on a VT1000X vibratome (Leica Microsystems, Buffalo Grove, Ill., USA) and stored at  $-20^{\circ}\text{C}$  in cryoprotectant (30% sucrose, 30% ethylene glycol in PB) until immunocytochemical processing.

Prior to each experiment, sections from the dorsal hippocampal [ $-3.5$  to  $-4.2$  mm from Bregma (Swanson, 1992)] sections were selected and rinsed in PB. To ensure identical labeling between groups, sections were coded with hole punches in the cortex and pooled into crucibles to be processed together throughout all immunocytochemical procedures (Pierce et al., 1999). Sections were incubated in 1% sodium borohydride in PB for 30 min to remove active aldehydes and then washed 8-10 times in PB until no gaseous bubbles remained.

### Antibody Characterization

All antibodies utilized in this experiment are the same as those employed in previous light and EM studies (Milner et al., 2013; Pierce et al., 2014; Mazid et al., 2016; Ryan et al., 2018; Bellamy et al., 2019; Reich et al., 2019; Ashirova et al., 2021).

**DOR:** A rabbit polyclonal antibody against amino acids 3-17 of DOR protein (Millipore Cat# AB1560, RRID: AB 90778) was utilized. As described previously (Mazid et al., 2016), the DOR antibody has been extensively characterized. Western blots of lysates from rat brains and NG108-15 cells, which endogenously express DORs (Barg et al., 1984; Persson et al., 2005; Saland et al., 2005), produced two major bands at 36kD and 72kD (representing dimer or glycosylated form of DOR). In preadsorption controls on lysates pre-incubated with 150  $\mu\text{g/ml}$  of immunogenic peptide and the antibody completely abolish

labeling (Persson et al., 2005). In preadsorption controls on tissue sections fixed with 4% paraformaldehyde, immunofluorescent labeling was eliminated (Olive et al., 1997). Furthermore, no detectable labeling of this antibody is seen in Western blots of COS-7 cells [see Supplemental Fig. 1 in (Williams et al., 2011a)], which do not endogenously express DORs (Kieffer et al., 1992) and in the dorsal raphe of DOR knockout mice [see Supplemental Fig. 1 in (Bie et al., 2010)]. The presence of DOR-immunoreactivity (-ir) with AB1560 in interneurons and pyramidal cells in the rat hippocampus is consistent with mRNA expression (Mansour et al., 1994; Johnson et al., 2020) and binding (Crain et al., 1986; Gulya et al., 1986; Mansour et al., 1987; McLean et al., 1987) for DOR in this species.

**LEnk:** A mouse monoclonal antibody to Leu<sup>5</sup>-Enkephalin (Sera labs; MAS 083p, clone NOCI, Lot P91G083; Crawley Down, UK) was employed in this study. This antibody recognizes LEнк, and to a lesser degree met-enkephalin and dynorphin, but not  $\beta$ -endorphin in immunoblots and adsorption controls (Milner et al., 1989).

**GABA:** A rat polyclonal antiserum selective against GABA- glutaraldehyde-hemocyanin conjugates (provided by Dr. Andrew Towle) was used. Specificity of this antibody has been validated in preadsorption control studies at a working dilution of 1:2000. Immunolabeling was completely abolished in 10  $\mu$ M soluble GABA- bovine serum albumin (BSA) conjugates but not blocked by unconjugated GABA or glutamate-, B-alanine-, taurine-conjugates (Lauder et al., 1986).

**MOR:** A rabbit polyclonal antibody (Neuromics Cat# RA10104-150, RRID: AB 2156526) that recognizes a 15-amino acid sequence (residues 384-398) in the C-terminus of MOR1 was utilized in this study. This antibody has been extensively characterized and does not recognize the splice variant MOR-1B-E or cloned DOR (Arvidsson et al., 1995; Abbadie et al., 2000). Specificity of this antibody has been demonstrated through Western blots from Neuro2a cells expressing MOR1 and rat brain tissue producing bands at 67-72 kDa (molecular weight). In adsorption control studies, immunolabeling was abolished following pre-incubation of a 1:2000 dilution of antibody with the antigenic peptide (MOR 384-398) (Arvidsson et al., 1995; Drake and Milner, 1999). Our previous study revealed that MOR- and PARV-ir are most commonly co-localized in the hilus of the rat dentate gyrus (Drake and Milner, 2006).

**PARV:** A mouse monoclonal PARV antibody (Millipore Sigma, Milwaukee, MI; Cat# P3088, RRID: AB\_477329) was used in this study. Specificity of this antibody has been demonstrated previously by its ability to recognize PARV in brain tissue at a working dilution of 1:5,000 by immunoblots and radioimmunoassay as well as preadsorption controls utilizing 100  $\mu$ l of working dilutions of 1:100 - 1:50,000 added to both antigenic and non-antigenic solutions (Celio et al., 1988; Celio, 1990).

**Phosphorylated DOR (pDOR):** A rabbit polyclonal antibody generated against a synthetic phosphopeptide corresponding to residues surrounding Ser363 of human pDOR (#3641 Cell Signaling, Danvers, MA) was used. Antibody specificity was characterized by Western blots done on hippocampal samples from wild-type mice producing a band at

65kDa but not DOR knock-out mice, 20 min following injection of the DOR agonist SNC80 (10 mg/kg) (Pradhan et al., 2009).

**Phosphorylated MOR (pMOR):** A rabbit polyclonal antibody generated against a synthetic phosphopeptide corresponding to residues surrounding Ser377 of human (homologous to Ser375 of mouse) pMOR (#3451 Cell Signaling, Danvers, MA, USA) was utilized in this study. Antibody specificity was characterized by Western blots of HEK293 cells and neuronal cells (Schulz et al., 2004). In immunoprecipitation studies of HEK293 cells and neuronal cells, immunolabeling of pMOR increased in the presence of the opioid receptor agonist DAMGO and decreased in the presence of the antagonist naloxone (Schulz et al., 2004). Furthermore, mutation of the Ser 375 residue of the MOR in HEK293 cells abolished morphine-induced phosphorylation (Chu et al., 2008). In absorption control studies, pMOR-ir was completely abolished in rat hippocampal sections (Gonzales et al., 2011).

### Light microscopic immunocytochemistry

**Immunolabeling procedures:** Free-floating hippocampal sections were processed for immunoperoxidase labeling using the avidin-biotin complex (ABC) protocol (Milner, 2011). Sections were sequentially incubated in: 1) 0.5% bovine serum albumin (BSA) in TS, 30 min.; 2) primary antisera (LEnk 1:1000 Dilution, pDOR, 1:800 dilution, pMOR, 1:800 dilution), in 0.1% BSA and 0.25% Triton-X in TS for 1 day at room temperature (~23°C), followed by 2 days in the cold (~4°C); 3) 1:400 dilution of either biotinylated donkey anti-mouse immunoglobulin (IgG; LENk; Vector Laboratories Cat# BA-2001; RRID:AB\_2336180) or goat-anti-rabbit IgG (pDOR, pMOR; Jackson ImmunoResearch Laboratories, Cat# 711-506-152, RRID: AB\_2616595) for 30 min.; and 4) ABC solution at half the manufacturer's recommended dilution (Vectastain Elite kit, Vector Laboratories, Burlingame, CA) in TS, 30 min. The bound peroxidase in the sections was visualized by a timed reaction (7 min LENk; 9 min pDOR; 11 min pMOR) in 3,3'-diaminobenzidine (DAB; Millipore Sigma) and hydrogen peroxide in TS. All incubation steps were separated by washes in TS. Incubations were carried out on a shaker at 145 rpm (antibodies) or at 90 rpm (washes). Sections were mounted on 1% gelatin-coated slides, dehydrated through an ascending series of alcohols and coverslipped from xylene with DPX mounting media (Cat. # 06522, Millipore Sigma).

**Analysis:** Optical densitometric analysis was performed by an experimenter blinded to conditional groups using previously described methods (Williams et al., 2011a). Light microscope photographs (10x) from each region of interest (ROI) were taken on a Nikon Eclipse 80i microscope using a Micropublisher 5.0 digital camera (Q-imaging, BC, Canada) and IP Lab software (Scanalytics IPLab, RRID:SCR\_002775). The mean density value was obtained using ImageJ64 (ImageJ, RRID:SCR\_003070) software for each ROI. For LENk, pixel density was determined from 6 ROIs: Crest, central hilus and dorsal blade of the dentate gyrus; stratum lucidum (SLu) of CA3a, b and stratum oriens (SO) of CA3a (Fig. 1a). For pMOR, pixel density was determined from 4 ROIs from CA3b: SO, pyramidal cell layer (PCL), SLu and stratum radiatum (SR). For pDOR, pixel density was obtained from 4 ROIs from CA2/3a: SO, PCL, SR medial, and SR distal. To control for variations in overall

illumination levels and background staining, the pixel density of an unlabeled tissue region was subtracted from the ROI pixel density measurements. Prior studies verified the accuracy of this method through a strong linear correlation between average pixel density and neutral density values of gelatin filters with defined transmittances ranging from 1 to 80% (Auchus and Pickel, 1992; Pierce et al., 1999; Pierce et al., 2014).

### Electron microscopic immunocytochemistry

**Immunolabeling procedures:** Free-floating hippocampal sections were dually labeled for DOR and GABA or MOR and PARV as previously described (Milner et al., 2013; Mazid et al., 2016). After rinsing in TS, sections were blocked in 0.5% BSA in TS for 30 min and then placed in a cocktail of either DOR (1:5000) + GABA (1:1000) or MOR (1:1000) + PARV (1:2500) in 0.1% BSA in TS. Sections were incubated for 24 hours at room temperature and then 4 days at 4°C. Next, sections were processed for immunoperoxidase labeling as described above except that either biotinylated donkey anti-rat IgG for GABA (Jackson ImmunoResearch Laboratories, Cat# 712-065-150, RRID: AB\_2340646) or biotinylated goat anti-mouse IgG for PARV (Vector Laboratories Cat# BA-2001; RRID: AB\_2827932) was used as a secondary antibody. Sections were placed in DAB in 3% H<sub>2</sub>O<sub>2</sub> in TS for 3 min (GABA) or 9 min (PARV).

Next, sections were processed for silver-intensified immunogold (SIG) labeling for DOR and MOR. For this, sections were rinsed in TS and incubated in donkey anti-rabbit IgG conjugated to 1-nm gold particles [diluted 1:50; EMS Cat# 810.311, RRID: AB\_25629850] in 0.01% gelatin and 0.08% BSA in 0.01 M phosphate-buffered Sal (PBS) at 4°C overnight. Sections then were rinsed in PBS, postfixed in 2% glutaraldehyde in PBS for 10 min and rinsed in PBS followed by 0.2 M sodium citrate buffer (SCB; pH = 7.4). IgG-conjugated gold particles were enhanced for 20 min (DOR) or 18 min (MOR) with silver solution (SEKL15 Silver enhancement kit, Prod No. 15718 Ted Pella Inc.), rinsed in SCB and then PB.

Sections were further processed for electron microscopy using previously described protocols (Milner, 2011). Sections were post-fixed in 2% osmium tetroxide in PB for 1 hr, followed by a dehydration series of alcohols and propylene oxide. Sections then were embedded in EMBed 812 (Electron Microscopy Sciences (EMS), Hatfield, PA, USA) between two sheets of Aclar plastic. Ultrathin sections (70 nm thick) through the ROI was cut with a diamond knife (EMS) on a UCT ultratome (Leica) and collected on 400-mesh thin-bar copper grids (T400-Cu, EMS). Sections were counterstained with Uranylless™ (EMS, #22409) for 2 min and lead citrate (EMS, #22410) for 1 min.

**Analysis:** All analyses were done by persons who were blind to experimental groups. Only females in proestrus and estrus (i.e., elevated estrogen levels) were chosen for analysis in the EM experiments. Ultrathin sections from 3 rats in each experimental condition was analyzed at the tissue-plastic interface to minimize the difference in antibody penetration (Milner, 2011). Photographs were taken on a Tecnai Biotwin or CM10 transmission electron microscope (FEI, Hillsboro, OR) and images were acquired with a digital camera system (v3.2, Advanced Microscopy Techniques, Woburn, MA). Immunolabeled profiles



were classified using defined morphological criteria (Peters et al., 1991). Briefly, dendritic profiles contain cytoplasm with mitochondria, microtubules, and agranular reticulum and were postsynaptic to axon terminal profiles identified by the presence of vesicles. Dendrites were further classified as either large (diameter  $>1.0\ \mu\text{m}$ ; i.e., proximal to cell body) or small (diameter  $<1.0\ \mu\text{m}$ ; i.e., distal to cell body). Larger dendrites are implicated in intraneuronal integration of inputs from multiple areas of the dendritic tree (Sjöström et al., 2008). Smaller dendrites are critical for coordinating excitatory neural transmission as they contain high levels of excitatory neurotransmitter receptors (London and Häusser, 2005). Dendritic spines were usually smaller than  $0.2\ \mu\text{m}$  in diameter, were contacted by terminals forming asymmetric synapses and are sometimes contiguous with dendritic shafts. Mossy fiber pathway terminals are identified by their large size ( $1\text{-}2\ \mu\text{m}$  in diameter) and often contact multiple dendritic spines of the CA3 pyramidal cell dendrites (Pierce et al., 2014). Peroxidase labeling of GABA- or PARV- dendritic profiles was identified as a dense precipitate appearing darker compared to non-labeled dendrites. SIG-labeling for DOR and MOR was identified as black dense particles (Milner et al., 2011).

**1. DOR-labeled CA3 dendrites:** Pyramidal cell dendrites containing DOR SIG labeling were photographed from SR of CA3b (Fig. 2a). A total of 50 random dendrites labeled with DOR only (labeled with SIG-particles but not immunoperoxidase for GABA) were photographed at a magnification of 13500x. Microcomputer imaging Device software (MCID) was used to determine the perimeter ( $\mu\text{m}$ ), cross-sectional area ( $\mu\text{m}^2$ ) and cross-sectional diameter of the dendrites. Subcellular localization of DOR-SIG particles were determined as either on plasmalemma (PM), near plasmalemma (near PM) or cytoplasmic (CY) (Fig. 2b). The density of DORs in dendrites was determined using the following parameters: (a) the number of SIG particles localized to the plasma membrane (PM: $\mu\text{m}$ ), (b) the number of SIG particles localized within 50 nm of the plasma membrane (Near PM: $\mu\text{m}$ ), (c) the number of SIG particles localized to the cytoplasm per cross-sectional area (CY: $\mu\text{m}^2$ ), and (d) the total number of SIG particles per cross-sectional area (Total: $\mu\text{m}^2$ ). The partitioning ratio of DORs was calculated as the proportion of SIG particles in a given subcellular compartment (on PM, near PM, or in the cytoplasm) divided by the total number of DOR-SIG particles within the dendrite. Dendrites were further classified as large (diameter  $> 1.0\ \mu\text{m}$ ) or small (diameter  $< 1.0\ \mu\text{m}$ ) based on average diameter measures.

The significance of SIG-particle labeling on the plasmalemma identifies receptor-binding sites, whereas SIG-particle labeling near the plasma membrane identifies a pool from which receptors can be added to or removed from the plasma membrane (Boudin et al., 1998). SIG-particle labeling in the cytoplasm identifies receptors that are either stored during transfer to or from the soma or another cellular component, or the receptors are being degraded or recycled (Pierce et al., 2009; Fernandez-Monreal et al., 2012). The functionality of receptor trafficking using SIG-particle labeling has been supported by the internalization of epitope-tagged MORs following morphine administration in the nucleus accumbens (Haberstock-Debic et al., 2003).

**2. DOR-labeled spines contacted by mossy fibers:** Fifty random mossy fibers which synapsed on dendrites within SLu were photographed per animal. All spines (labeled and

unlabeled) contacted by the mossy fibers were tallied and subcellular locations (synapse, plasmalemma, cytoplasmic) were noted. The percent of DOR-labeled spines was calculated by dividing the number of DOR labeled spines over the total number of spines.

**3. DOR-labeled spines in SR of CA3.:** From the SR micrographs collected in analysis 1, 100 dendritic spines were randomly identified and tallied. If the spines contained DOR-labeled particles, the percent labeled was calculated and the subcellular distribution (synapse, plasmalemma, cytoplasm) was noted.

**4. MOR/PARV dendrites in the dentate gyrus.:** In the hilus of the dentate gyrus, 50 dually labeled MOR/PARV interneuron dendrites were photographed. The density of MOR SIG particles and partitioning ratio within PARV-labeled dendrites was determined as described above in analysis 1 for DOR dendrites.

**Figure preparation.**—As the EM results represent a statistical analysis of many micrographs, it is challenging to select a single micrograph that reflects all of the DOR or MOR distribution changes within the dendrites seen in the graphs. Thus, the micrographs were selected so that the distribution of the SIG particles in the four groups reflected the data without contradicting it.

Light and electron micrographs were adjusted for brightness, sharpness and contrast on Adobe Photoshop 2020 (Adobe Photoshop, RRID:SCR\_014199). Images then were imported into Microsoft Powerpoint [version 16.16.18 (200112)] where final adjustments to brightness, sharpness, and contrast were performed. Adjustments were done to the entire image to achieve uniformity in appearance between micrographs and did not alter the original content of the raw image. Graphs were generated using Prism 8 software (GraphPad Prism, La Jolla, CA; RRID:SCR\_002798).

**Statistical analysis.**—Data are expressed as means  $\pm$  SEM. Significance was set to an alpha  $< 0.05$ . Statistical analyses were conducted on JMP 12 Pro software (JMP, RRID:SCR\_014242). For light microscopic densitometry studies (LEnk, pMOR, pDOR), a Student's *t*-test was used for two group comparisons to identify estrus cycle effects, vehicle (baseline) differences and treatment (THC) effects in females and males. For EM studies, a two-way analysis of variance (ANOVA) was used for comparing dendritic labeling across all groups analyzing for main effects of “sex” or “treatment” and interactions effects of “sex by treatment” followed by a post-hoc Tukey HSD. A student's *t*-test was used to do two group comparisons of labeled spines identifying baseline differences and treatment effects in females and males.

For EM analyses, our prior studies determined that 50 dendrites on average were sufficient to make quantitative comparisons on the subcellular distribution of proteins (Znamensky et al., 2003). This approach for analysis has been employed by numerous studies from our laboratory as well as other laboratories (Bangasser et al., 2010; Marques-Lopes et al., 2014; Mazid et al., 2016; McAlinn et al., 2018).

## RESULTS

### Mossy fiber LEnk levels are affected by acute THC in proestrus/estrus females

Consistent with previous studies (Torres-Reveron et al., 2008; Pierce et al., 2014), diffuse LEnk-immunoreactivity (ir) was found in the hilus of the dentate gyrus and in SLu of CA3 (i.e., the mossy fiber pathway; Fig. 1A). Moreover, scattered LEnk-ir labeling is also present in SO of CA3. Optical density of LEnk labeling first was measured from mossy fiber subregions in CA3a, CA3b and the dentate gyrus (DG) in females (without regard to estrous cycle stage) and males following VEH or THC (Fig. 1A). No significant differences in the density of LEnk-ir was noted between any groups in any of the regions in the CA3 or the dentate gyrus.

As prior studies have demonstrated that mossy fiber LEnk levels are elevated when estrogen levels are highest (Torres-Reveron et al., 2008; Pierce et al., 2014), females were further divided based on estrus cycle stage. We found that VEH proestrus/estrus females compared to VEH diestrus females tended to have higher LEnk-labeling in the SLu of CA3a [ $t(2.98)=2.84$ ;  $p=0.06$ ] (Fig. 1D). Additionally, THC females (all proestrus/estrus) tended to have decreased LEnk labeling in the SLu of the CA3a [ $t(19)=1.81$ ;  $p=0.08$ ] compared their VEH proestrus/estrus counterparts (Fig. 1B-D). These findings suggest that acute THC decreases the mossy fiber LEnk levels in females with elevated estrogen levels.

### Acute THC differentially alters the distribution of DORs in CA3 dendrites in females and males

EM studies examined the distribution of DORs in CA3b pyramidal cell dendrites (analysis 1). Representative micrographs of DOR-SIG labeling in large dendrites are shown for VEH- and THC-injected females and males in Figure 3. Consistent with prior studies (Mazid et al., 2016; Ryan et al., 2018; Ashirova et al., 2021), CA3 dendrites often have multiple spines contacted by terminals forming asymmetric synapses (examples, Fig. 3A, B).

The density of DOR-SIG particles within CA3 dendrites from the females and males following THC injections first were analyzed without consideration of size. Two-way ANOVA did not show any significant differences across groups in any subcellular compartment. However, an additional Students *t*-test showed that THC-Females tended [ $t(596)=-1.92$ ;  $p=0.06$ ] to have a reduction in the density of DOR-SIG near the plasmalemma compared to VEH-females (not shown).

Next, DOR-labeled dendrites were analyzed based on size. In *large CA3 dendrites*, two-way ANOVA did not show any significant differences across groups in DOR-SIG labeling on or near the plasmalemma. However, a student's *t*-test revealed that VEH-males compared to VEH-females tended [ $t(322)=-1.76$ ;  $p=0.08$ ] to have a decreased density of DOR SIG particles near the plasmalemma of large CA3 dendrites. Additionally, THC-males compared to VEH-males had a greater density of near plasmalemmal DOR-SIG particles [ $t(322)=-2.04$ ;  $p=0.04$ ] in large CA3 dendrites (Fig. 4A). Within the cytoplasm, two-way ANOVA comparing across all groups shows a main effect of treatment [ $F(1,322)=4.41$ ;  $p=0.04$ ]. Post-hoc Tukey confirms that THC-females compared to VEH-females had reduced density ( $p=0.03$ ) of cytoplasmic DOR-SIG labeling in large CA3 dendrites (Fig. 4B).

An additional student *t*-test also shows that a treatment effect was only seen in females. THC-females compared to VEH-females have a reduced density of cytoplasmic DOR-SIG particles in large CA3 dendrites [ $t(322)=2.83$ ;  $p=0.005$ ]. Two-way ANOVA also show an interaction effect of sex by treatment [ $F(1,322)=8.41$ ;  $p=0.004$ ] on the total density of DOR-SIG labeling in large CA3 dendrites. Post-hoc Tukey shows that VEH-females compared to VEH-males have a significantly ( $p=0.04$ ) greater total DOR-SIG particle density in large CA3 dendrites. Post-hoc Tukey also shows that THC-females compared to VEH-females have a significant reduction ( $p=0.002$ ) in DOR-SIG labeling in large CA3 dendrites (Fig. 4B).

In small CA3 dendrites, two-way ANOVAs did not show any differences across groups of DOR density on the plasmalemma or cytoplasm. However, two-way ANOVA showed an interaction effect of sex by treatment on the density of DORs near the plasmalemma [ $F(1,270)=7.30$ ;  $p=0.007$ ] and in total [ $F(1,270)=7.67$ ;  $p=0.006$ ] of small dendrites. Post-hoc Tukey shows THC-females compared to VEH-females had a significantly higher density of near plasmalemmal ( $p=0.04$ ) and total ( $p=0.02$ ) DOR-SIG particles in small dendrites (Fig. 4C). An additional student's *t*-test showed that VEH-females compared to VEH-males had significantly less [ $t(270)=2.31$ ;  $p=0.02$ ] total DOR-SIG density in small dendrites. There were no differences in DOR-SIG distribution in any cellular compartment in small dendrites in males (Fig. 4D).

In analysis of partitioning ratios of DOR-SIG particles, dendrites were first analyzed without consideration to size. However, two-way ANOVA showed no significant differences in the proportion of on, near or cytoplasmic DORs across groups. Next, partitioning ratios of DORs were analyzed separately in large and small dendrites. In large dendrites, two-way ANOVA showed a main effect of sex on DOR-SIG particles on the plasmalemma [ $F(1,322)=4.11$ ;  $p=0.04$ ]. However, both post-hoc Tukey as well as additional student's *t*-tests did not show any significant differences between the groups. Two-way ANOVA shows a main effect of treatment on the ratio of DORs near the plasmalemma [ $F(1,322)=5.76$ ;  $p=0.02$ ] and in the cytoplasm [ $F(1,322)=4.21$ ;  $p=0.04$ ] of large CA3 dendrites. Post-hoc Tukey showed that THC-males compared to VEH-males had a significant increase ( $p=0.05$ ) in the ratio of DOR-SIG particles near the plasmalemma of large dendrites (Fig. 4F). In females, there were no significant differences in any of the partitioning ratios for DORs in large dendrites (Fig. 4E). Although post-hoc Tukey for cytoplasmic DORs was not significant, a student's *t*-test showed that THC-males compared to VEH-males had significantly lower cytoplasmic ratio [ $t(322)=2.46$ ;  $p=0.01$ ] of DOR-SIG particles in large CA3 dendrites (Fig. 4F). In small dendrites, there was no significant difference in the ratio of DORs in any compartment between the groups.

These findings demonstrate that females compared to males at baseline have an overall greater reserve of DORs in proximal (large) CA3 dendrites. Moreover, acute THC in both females and males redistributes DORs to readily releasable pools (near plasmalemma) in CA3 dendrites (albeit in different locations within the dendritic tree). Thus, these results suggest acute THC redistributes DORs in CA3 dendrites in a manner that would promote synaptic plasticity in both sexes upon exposure to opioid ligands.

### Following acute THC, DOR-labeled mossy fiber-CA3 synapses decrease in males

In agreement with prior studies (Harte-Hargrove et al., 2015; Mazid et al., 2016; Ryan et al., 2018; Ashirova et al., 2021), DOR-labeling was found in CA3 pyramidal cell dendritic spines in SLu and SR. Representative micrographs showing DOR labeling in CA3 dendritic spines contacted by mossy fibers terminals in SLu (i.e., mossy fiber-CA3 synapses) and within SR are shown in Figure 5. The percentage and number of DOR-labeled spines in both SLu and SR are summarized in Table 1.

There were no significant differences in the percentage of DOR-labeled mossy fiber-CA3 synapses between VEH-females and VEH-males. However, the percentage and number of DOR-labeled spines in SR tended to be greater [ $t(2.30)=-3.20$ ;  $p = 0.07$ ] in VEH-females compared to VEH-males. In both SLu and SR, VEH-females had about twice as many DOR-SIG particles on the synapse and near the plasma membrane compared to VEH-males. However, VEH-females compared to VEH-males had about one-third fewer DOR-SIGs in the cytoplasm of mossy fiber-CA3 synapses and about twice as many cytoplasmic DOR SIGs in SR spines.

THC-males compared to VEH-males had a significantly reduced percentage [ $t(2.96)=3.11$ ;  $p = 0.05$ ] of DOR-SIG labeled mossy fiber-CA3 synapses. Moreover, THC-females compared to THC-males had significantly greater percentage and number [ $t(3.13)=3.40$ ;  $p = 0.04$ ] of DOR-labeled spines in SR.

Collectively with the results above in DOR dendrites, these findings suggest that DORs traffic from the dendritic spines to the near plasmalemma of dendritic shafts in males.

### In the dentate gyrus, acute THC decreases near-plasmalemmal MORs in PARV interneuron dendrites in males

Prior studies (Torres-Reveron et al., 2009; Milner et al., 2013) have shown that MOR-SIG labeling is co-localized with PARV in interneurons primarily found in the subgranular zone in the hilus of the dentate gyrus. Representative electron micrographs showing dendrites dually labeled for MOR-SIG and PARV-immunoperoxidase from each experimental group are presented in Figure 6A-D. MOR/PARV labeled dendrites in both VEH- and THC-injected female and male rats do not contain spines and are contacted by numerous terminals forming asymmetric synapses.

Analysis was first performed without consideration of size. Two-way ANOVA comparing across groups revealed no significant differences in MOR density in any subcellular compartment (i.e., on and near the plasmalemma, cytoplasm or in total) of PARV-labeled dendrites. However, a student t-test showed that THC-males compared to VEH-males tended [ $t(596) = -1.77$ ;  $p = 0.07$ ] to have a greater density of MOR-SIG particles within the cytoplasm of PARV dendrites (Fig. 7A, B).

In *large PARV dendrites*, two-way ANOVA showed an interaction effect of sex by treatment [ $F(1, 216) = 6.15$ ;  $p = 0.01$ ] on the plasmalemma. Post-hoc Tukey showed that THC-males compared to VEH-males have a significantly lower ( $p = 0.03$ ) density of MORs on the plasmalemma of large PARV dendrites (Fig. 7D). No significant differences in MOR

densities are seen in any other subcellular compartment in males or in females (Fig. 7C). In *small PARV dendrites*, two-way ANOVA showed no differences across groups in any subcellular compartment. However, student t-tests showed that THC-males compared to VEH-males tended [ $t(376)=-1.88$ ;  $p = 0.07$ ] to have a higher density of cytoplasmic MOR-SIG labeling in small PARV dendrites (not shown).

Two-way ANOVA analysis of partitioning ratios of MOR-SIG particles in PARV dendrites without consideration of size showed no significant differences across groups in any subcellular compartment. However, student t-tests showed THC-males compared to VEH-males had a lower ratio [ $t(596) = 1.97$ ;  $p = 0.05$ ] of MOR-SIG particles on the plasma membrane of PARV dendrites (not shown). In *large PARV dendrites*, two-way ANOVA showed an interaction effect of sex and treatment [ $F(1, 216) = 4.99$ ;  $p=0.03$ ]. Post-hoc Tukey confirmed that THC-males compared to VEH-males had a significantly lower ratio ( $p = 0.03$ ) of MOR-SIG particles on the plasmalemma of large PARV dendrites (Fig. 7F). Additionally, t-tests show that THC females tended to have a higher ratio of MOR-SIG particles near the plasmalemma compared to VEH females [ $t(592) = 1.77$ ;  $p=0.08$ ] and reduced MOR-SIG particles in the cytoplasm compared to VEH females [ $t(597) = 1.88$ ;  $p=0.06$ ; Fig. 7E] In the *small PARV dendrites*, no significant differences were found in the ratio of MORs in PARV dendrites in any subcellular compartment via ANOVAs or student t-tests.

Thus, these findings demonstrate that acute THC reduces pools of MORs available for ligand binding on PARV interneurons in adult males, but not females.

### **Acute THC increases pMOR in CA3 of females with elevated estrogen levels**

As shown in our prior studies (Gonzales et al., 2011; Bellamy et al., 2019), diffuse pMOR-ir was found primarily in SLu of CA3, and to a lesser extent in SO, PCL and SR (Fig. 8A). In most CA3b lamina pMOR levels were altered by estrous cycle phase in VEH-females. Specifically, the density of pMOR-ir was higher in diestrus VEH-females compared to proestrus/estrus VEH-females in SO [ $t(2.78) = 4.28$ ;  $p = 0.03$ ], the PCL [ $t(3.98) = 2.618$ ;  $p = 0.06$ ] and SR [ $t(3.53) = 5.53$ ;  $p = 0.007$ ] of CA3b (Fig. 8B-E). Furthermore, proestrus/estrus VEH-females compared to VEH-males had significantly lower density of pMOR-ir in CA3b SO [ $t(6.99) = 4.53$ ;  $p = 0.002$ ], the PCL [ $t(5.23) = 2.70$ ;  $p = 0.04$ ] and SR [ $t(6.877) = 3.07$ ;  $p = 0.02$ ]. A treatment effect was seen only in females. Specifically, THC-females compared to proestrus/estrus VEH-females had a higher density of pMOR-ir in SO [ $t(6.702) = 3$ ;  $p = 0.02$ ], the PCL [ $t(4.925) = 2.95$ ;  $p = 0.03$ ] and SR [ $t(6.905) = 4.20$ ;  $p = 0.004$ ] of CA3b. Thus, following acute THC, pMOR levels increased in most CA3b lamina in proestrus/estrus females so that they were similar to those observed in diestrus VEH-females and males.

### **Acute THC increases pDOR in CA2/3a pyramidal cell dendrites of females with elevated estrogen levels**

Consistent with our earlier studies (Burstein et al., 2013; Bellamy et al., 2019), density of pDOR-ir is highest in the PCL, SO and SR of CA2/3a (Fig. 9A). For the analysis, SR was further divided into 2 regions denoted as “proximal SR” (i.e., within 100  $\mu\text{m}$  of the PCL layer) and “distal SR” (i.e., >100  $\mu\text{m}$  from the PCL layer).

Baseline differences in the density of pDOR-ir in CA2/3a was seen in some lamina. In VEH injected rats, diestrus females compared to PE/E females tended [ $t(2,373)=-3.15$ ;  $p=0.07$ ] to have higher pDOR labeling within the proximal SR of CA2/3a (Fig. 9D). Moreover, PE/E VEH-females compared to VEH-males had significantly lower pDOR labeling in the PCL [ $t(17)= 2.28$ ;  $p=0.04$ ], proximal SR [ $t(17)= 3.25$ ;  $p= 0.0005$ ] and distal SR [ $t(17)= 2.82$ ;  $p= 0.01$ ] of CA2/3a. A treatment effect was seen in only females. THC-females compared to VEH-females had significantly higher [ $t(17)= -2.41$ ;  $p=0.03$ ] pDOR labeling in the proximal SR of CA2/3a (Fig. 9B-D).

Prior EM studies show that the majority of pDOR-labeling in SR of CA2/3a is found in pyramidal cell dendrites (Burstein et al., 2013). Thus, these findings indicate that acute THC increased pDOR levels in CA2/3a pyramidal cell dendrites in females in elevated estrogen states to that seen in males.

## DISCUSSION

This study shows a sex-dependent alteration in the hippocampal opioid system after a single dose of THC. In females with elevated estrogen states, acute THC altered the opioid system so that it resembled that seen in vehicle-injected females with low estrogen states and males. In males, acute THC resulted in the internalization of MORs in parvalbumin-containing hilar interneuron dendrites which would decrease disinhibition of granule cells. However, acute THC also resulted in a sex-specific redistribution of DORs within CA3 pyramidal cell dendrites which could differentially increase synaptic plasticity and/or opioid-associated learning processes in females and males.

### Methodological considerations

As in our prior studies (Ryan et al., 2018; Reich et al., 2019; Ashirova et al., 2021), a single cohort of animals was used to minimize potential environmental and handling confounds. However, as vehicle-injected females were in different estrous phases, we divided the light microscopic data into high (PE/E) and low (DE) estrogen groups. Despite the reduced statistical power for the light microscopy experiments, the findings presented here are generally consistent with prior studies.

The moderate THC dose of 5 mg/kg was selected as it produces roughly equivalent peak plasma THC concentrations and total drug exposure in male and female rats as those observed in humans following voluntary cannabis inhalation (Huestis et al., 1992; Cooper and Haney, 2009; Ruiz et al., 2020). Similar plasma THC concentrations have been observed for a range of THC doses in rats across sex, ages, and strains (Narimatsu et al., 1991; Tseng et al., 2004; Wiley and Burston, 2014; Craft et al., 2019; Ruiz et al., 2020). However, despite the similar plasma and brain levels of THC, sex dependent differences in THC metabolism have been demonstrated (Narimatsu et al., 1991; Britch et al., 2017; Wiley et al., 2021). Adolescent and adult males metabolize THC via cytochrome P450 2C11 (CYP2C11) into several metabolites including the active metabolite 11-hydroxy-9-THC (11-OH-THC) while female rats have been shown to preferentially metabolize THC via CYP2C6 into 11-OH-THC (Narimatsu et al., 1990; Narimatsu et al., 1991; Narimatsu et al., 1992; Tseng et al., 2004; Craft et al., 2019). Despite similar plasma THC levels in male and female rats,

female rats have increased circulating levels of 11-OH-THC compared to males (Tseng et al., 2004; Craft et al., 2019). Since 11-OH-THC, similar to THC, is a partial agonist with slightly higher affinity (~1.5 fold) for CB1 receptors in both sexes of rat (Wiley et al., 2021), the observed subcellular trafficking differences in the hippocampal opioid system following acute 5 mg/kg THC may be due in part to increased cannabimimetic effects of this active metabolite.

### Baseline sex differences in opioid system

Our finding that VEH high estrogen (PE/E) females compared to VEH low estrogen (DE) females have higher levels of LENk in SLu of CA2/3a is consistent with prior studies (Torres-Reveron et al., 2008; Pierce et al., 2014). Moreover, our finding that VEH females with elevated estrogen levels compared to VEH males have significantly more near plasmalemma DORs in large CA3 dendrites is also congruent with previous studies (Mazid et al., 2016).

In the stratum radiatum of the CA3, more DOR labeled spines were seen in VEH females compared to VEH males. Furthermore, in the SLu, VEH females compared to VEH males showed more DORs present in the synapse of dendritic spines. Together, these results support our prior studies that mossy fiber LENk levels and DORs in CA3 pyramidal cells are positioned in drug-naïve high estrogen females to promote opioid dependent LTP (Harte-Hargrove et al., 2015).

The present studies also observed a significant reduction in baseline pMOR-ir labeling in most lamina of CA3b in VEH PE/E females compared to VEH DE females and males. These findings contrast our prior studies (Gonzales et al., 2011; Bellamy et al., 2019; Ashirova et al., 2021) which found no sex or estrous cycle differences in pMOR levels in CA3 or dentate gyrus in uninjected or saline-injected rats. Moreover, the VEH PE/E females compared to VEH DE females and males had less pDOR-ir in some lamina of CA2/CA3a. However, prior studies have shown increased CA2/CA3a pDOR-ir in uninjected or saline-injected E females compared to DE females or male rats (Burstein et al., 2013; Ashirova et al., 2021). Phosphorylation of MORs and DORs is important for uncoupling and internalization of activated receptors (Pradhan et al., 2009). The observed differences in pMOR and pDOR levels in the present study and prior studies may be due to the Tween 80 vehicle used for the THC experiments. An excipient or solubilizing agent is required for THC due to its poor aqueous solubility. Water-soluble non-ionic solubilizers/surfactants, such as Tween 80, have been shown *in vitro* to inhibit hERG potassium currents and *in vivo* to alter gastrointestinal, renal, and liver function in rats as well as plasma lipoproteins in mice (Woodburn and Kessel, 1994; Pestel et al., 2006; Himmel, 2007). Moreover, estrogen has been shown to influence lipoproteins (Parini et al., 2000), therefore it is possible that the observed reductions in phosphorylated receptors in PE/E females was due to an estrogen mediated effect of Tween 80 on lipoproteins.

### Female specific alterations in the hippocampal opioid system following acute THC

In females with elevated estrogen states, acute THC altered the opioid system so that it resembled that seen in VEH-injected females with low estrogen states and males: 1) mossy



fiber LEnk levels in CA2/3a decreased; 2) phosphorylated-DOR levels in CA2/3a pyramidal cells increased; 3) phosphorylated-MOR levels increased in CA3b laminae except SLu; and 4) cytoplasmic and total DORs in CA3b pyramidal cell dendrites decreased.

Although mossy fiber LEnk levels are elevated at high estrogen states (Torres-Reveron et al., 2008), our prior studies have shown that acute stress reduces mossy fiber LEnk-ir labeling (Pierce et al., 2014). Thus, similar to stress, acute THC may eliminate the estrogen effects on mossy fiber LEnk levels. Furthermore, following THC, the percent of DOR-labeled spines in SLu are unchanged. Together, these findings suggest that THC-injected females may have a reduced capacity for opioid-mediated LTP in mossy fiber-CA3 synapses (Harte-Hargrove et al., 2015).

For many receptors, including DORs and MORs, ligand binding initiates the phosphorylation of the receptors which results in the uncoupling and internalization of the receptor (Pradhan et al., 2009; Dang and Christie, 2012). Our prior studies have shown that pDORs are located near the plasma membrane and at postsynaptic densities of CA2 pyramidal cells (Burststein et al., 2013). Additionally, we have shown that pMORs are located in dendritic shafts of CA3 pyramidal cells (Gonzales et al., 2011). Thus, these findings suggest that the increase in both pDOR and pMOR in the CA3 following acute THC would result in a desensitization of DORs and MORs in CA3 pyramidal cells.

### **Male specific changes in the hippocampal opioid system following acute THC**

In contrast to females, acute THC in males had no effect on the levels of LEnk, pDOR or pMOR within the CA3 region. Additionally, acute THC in males, but not females, yields an internalization of MORs in parvalbumin-containing hilar GABA-interneuron dendrites. This decrease of MORs on the plasmalemma following acute THC would reduce pools of MORs available for ligand binding (Boudin et al., 1998) on PARV interneurons in adult males. Activation of MORs on GABAergic interneurons leads to the disinhibition (i.e., activation) of granule cells which can increase the release of endogenous LEnk from mossy fibers and subsequently increase LTP in CA3 pyramidal cells (Drake et al., 2007; Harte-Hargrove et al., 2015). Thus, acute THC in males would potentially reduce these processes.

### **Acute THC redistributes DORs in CA3 pyramidal cells in a sex-specific manner**

In both females and males, acute THC altered the distribution of DORs in CA3 pyramidal cells, however, the region of the dendrites in which DORs were redistributed varied with sex. In females, acute THC decreased cytoplasmic and overall total DORs in large CA3 dendrites and this was accompanied by an increase in near plasmalemma DORs in small CA3 dendrites. In contrast, acute THC in males decreased DORs in mossy fiber - CA3 synapses and increased near plasmalemma DORs in large CA3 pyramidal cell dendrites. This sex difference in the redistribution of DORs within CA3 pyramidal cells could have different influences on synaptic plasticity processes in females and males. While both large (proximal) and small (distal) dendrites receive excitatory inputs, large dendrites usually receive inputs from local sources whereas smaller dendrites integrate inputs from distant locations (London and Häusser, 2005; Spruston, 2008). Thus, in females, acute THC increased DORs on distal dendrites that would be post-synaptic to entorhinal cortical

Author Manuscript

afferents, many of which contain LENk (Drake et al., 2007). As perforant path projections to the CA3 promote both NMDA- and opioid-mediated LTP (Do et al., 2002), elevated DORs in distal CA3 dendrites would influence these processes in females following acute THC. In males, acute THC increased DORs in the proximal dendrites which are postsynaptic to “autoassociative” recurrent collaterals of CA3 cells (Scharfman and MacLusky, 2017). As autoassociative function of CA3 neurons are thought to be important for pattern separation and completion which are features of episodic memory (Scharfman and MacLusky, 2017), elevated DORs in proximal dendrites in males may promote these processes. However, as DORs also decreased in mossy fiber-CA3 synapses with acute THC, mechanisms promoting opioid receptor LTP at these synapses (Breindl et al., 1994; Harte-Hargrove et al., 2015) would be expected to be concurrently decreased.

Author Manuscript

The redistribution of DORs within CA3 pyramidal cell dendrites following acute THC could also influence plasticity and neuroprotective processes in response to stress involving other G protein coupled receptors. In particular, CA3 pyramidal cells contain both DOR and corticotropin releasing factor type 1 receptors (CRFR1) (McAlinn et al., 2018) which are known to utilize common signaling pathways including protein kinase C and mitogen-activated protein kinase (Battaglia et al., 1987; Quock et al., 1999; Blank et al., 2003; Hillhouse and Grammatopoulos, 2006). Additionally, DOR agonists can attenuate CRFR1 induced production of intracellular cyclic AMP (Williams et al., 2011b). Thus, the increase of DORs in CA3 pyramidal dendrites seen following acute THC could alter the balance of DOR/CRFR1 in both females and males in favor of DORs leading to a greater reduction in cyclic AMP production. In support, our prior EM studies have shown that baseline numbers of plasmalemmal DORs and CRFR1s in CA3 pyramidal cell dendrites are higher in males compared to females (Mazid et al., 2016; McAlinn et al., 2018), and thus, the elevation of DORs following acute THC may have a more profound effect in males. For example, as CRFR1 activation decreases glutamate mediated excitotoxicity of pyramidal neurons via cyclic AMP-dependent mechanisms (Hollrigel et al., 1998; Elliott-Hunt et al., 2002), elevated DORs, could inhibit neuroprotective effects of CRF in response to stress, especially in males.

Author Manuscript

The increased presence of available pools of DORs for ligand binding on CA3 pyramidal cells following acute THC could also have implications for opioid addictive processes. In male rats, disruption of morphine CPP following administration of a DOR antagonist is associated with an increased DOR dimer expression in post-synaptic densities in hippocampal tissue (Billa et al., 2010). Additionally, chronic morphine use, in which MORs are desensitized (Bailey and Connor, 2005), leads to an increased importance of DORs for endogenous and exogenous opioid signaling in the CA3. Thus, the redistributions of DORs to the near plasma membrane seen following acute THC would further favor the enhancement of DOR mediated processes following chronic opioid use.

### Prospective

Author Manuscript

The present study focused on the effects of acute THC on the hippocampal opioid system, however, little is known regarding the long-term adaptations of the hippocampal opioid system to chronic THC. Evidence from the human literature indicates that increased self-

exposure to non-medical cannabis use by teens and young adults is a positive predictor of opioid dependence diagnosis (Butelman et al., 2018a). Moreover, although self-exposure to cannabis is still apparently higher in men than women (Butelman et al., 2018b; Cooper and Craft, 2018), adolescent and adult females show an accelerated course of problematic cannabis use (Hernandez-Avila et al., 2004; Ehlers et al., 2010; Schepis et al., 2011). As the hippocampal opioid system is important for spatial memory and in contextual associative learning (Meilandt et al., 2004; Kesner and Warthen, 2010), determining the effects of chronic THC on the opioid system in adolescents and adults could have important clinical implications.

## Acknowledgements

Supported by NIH grants DA08259 (T.A.M., M.J.K., B.S.M.), HL098351 (T.A.M.), HL 136520 (T.A.M.), and MH041256 (B.S.M.), the Hope for Depression Research grant (B.S.M.), the Gary R. Helman Postdoctoral Research Fellowship (K.A.W), and the Dr. Miriam and Sheldon G. Adelson Medical Research Foundation (M.J.K.). We thank Ms. June Chan and Dr. Diane Lane for technical assistance.

## Data availability:

Data available on request from the authors.

## REFERENCES

- Abbadie C, Pan Y, Drake CT, Pasternak GW (2000) Comparative immunohistochemical distributions of carboxy terminus epitopes from the mu-opioid receptor splice variants MOR-1D, MOR-1 and MOR-1C in the mouse and rat CNS. *Neuroscience* 100:141–153. [PubMed: 10996465]
- Arvidsson U, Riedel M, Chakrabarti S, Lee JH, Nakano AH, Dado RJ, Loh HH, Law PY, Wessendorf MW, Elde R (1995) Distribution and targeting of a mu-opioid receptor (MOR1) in brain and spinal cord. *J Neurosci* 15:3328–3341. [PubMed: 7751913]
- Ashirova E, Contoreggi NH, Johnson MA, Al-Khayat FJ, Calcano GA, Rubin BR, O'Conneide EM, Zhang Y, Zhou Y, Gregoire L, McEwen BS, Kreek MJ, Milner TA (2021) Oxycodone injections not paired with conditioned place preference have little effect on the hippocampal opioid system in female and male rats. *Synapse* 75:e22182. [PubMed: 32654187]
- Auchus AP, Pickel VM (1992) Quantitative light microscopic demonstration of increased pallidal and striatal met5-enkephalin-like immunoreactivity in rats following chronic treatment with haloperidol but not with clozapine: implications for the pathogenesis of neuroleptic-induced movement disorders. *Exp Neurol* 117:17–27. [PubMed: 1618284]
- Bailey CP, Connor M (2005) Opioids: cellular mechanisms of tolerance and physical dependence. *Curr Opin Pharmacol* 5:60–68. [PubMed: 15661627]
- Bangasser DA, Curtis A, Reyes BA, Bethea TT, Parastatidis I, Ischiropoulos H, Van Bockstaele EJ, Valentino RJ (2010) Sex differences in corticotropin-releasing factor receptor signaling and trafficking: potential role in female vulnerability to stress-related psychopathology. *Mol Psychiatry* 15:877, 896–904. [PubMed: 20548297]
- Barg J, Levy R, Simantov R (1984) Up-regulation of opiate receptors by opiate antagonists in neuroblastoma-glioma cell culture: the possibility of interaction with guanosine triphosphate-binding proteins. *Neurosci Lett* 50:133–137. [PubMed: 6093009]
- Battaglia G, Webster EL, De Souza EB (1987) Characterization of corticotropin releasing factor receptor mediated adenylate cyclase activity in the rat central nervous system. *Synapse (New York, NY)* 1:572–581.
- Bellamy JR, Rubin BR, Zverovich A, Zhou Y, Contoreggi NH, Gray JD, McEwen BS, Kreek MJ, Milner TA (2019) Sex and chronic stress differentially alter phosphorylated mu and delta opioid receptor levels in the rat hippocampus following oxycodone conditioned place preference. *Neuroscience letters*:134514. [PubMed: 31560995]

- Bie B, Zhang Z, Cai YQ, Zhu W, Zhang Y, Dai J, Lowenstein CJ, Weinman EJ, Pan ZZ (2010) Nerve growth factor-regulated emergence of functional delta-opioid receptors. *J Neurosci* 30:5617–5628. [PubMed: 20410114]
- Billa SK, Liu J, Bjorklund NL, Sinha N, Fu Y, Shinnick-Gallagher P, Morón JA (2010) Increased insertion of glutamate receptor 2-lacking alpha-amino-3-hydroxy-5-methyl-4-isoxazole propionic acid (AMPA) receptors at hippocampal synapses upon repeated morphine administration. *Mol Pharmacol* 77:874–883. [PubMed: 20159947]
- Blank T, Nijholt I, Grammatopoulos DK, Randeve HS, Hillhouse EW, Spiess J (2003) Corticotropin-releasing factor receptors couple to multiple G-proteins to activate diverse intracellular signaling pathways in mouse hippocampus: role in neuronal excitability and associative learning. *The Journal of neuroscience : the official journal of the Society for Neuroscience* 23:700–707. [PubMed: 12533630]
- Bonilla-Del Río I, Puente N, Mimenza A, Ramos A, Serrano M, Lekunberri L, Gerrikagoitia I, Christie BR, Nahirney PC, Grandes P (2020) Acute 9-tetrahydrocannabinol prompts rapid changes in cannabinoid CB(1) receptor immunolabeling and subcellular structure in CA1 hippocampus of young adult male mice. *J Comp Neurol*.
- Boudin H, Pelaprat D, Rostene W, Pickel VM, Beaudet A (1998) Correlative ultrastructural distribution of neurotensin receptor proteins and binding sites in the rat substantia nigra. *J Neurosci* 18:8473–8484. [PubMed: 9763490]
- Breindl A, Derrick BE, Rodriguez SB, Martinez JL Jr. (1994) Opioid receptor-dependent long-term potentiation at the lateral perforant path-CA3 synapse in rat hippocampus. *Brain Res Bull* 33:17–24. [PubMed: 8275323]
- Britch SC, Wiley JL, Yu Z, Clowers BH, Craft RM (2017) Cannabidiol-Delta(9)-tetrahydrocannabinol interactions on acute pain and locomotor activity. *Drug Alcohol Depend* 175:187–197. [PubMed: 28445853]
- Brusco A, Tagliaferro P, Saez T, Onaivi ES (2008a) Postsynaptic localization of CB2 cannabinoid receptors in the rat hippocampus. *Synapse* 62:944–949. [PubMed: 18798269]
- Brusco A, Tagliaferro PA, Saez T, Onaivi ES (2008b) Ultrastructural localization of neuronal brain CB2 cannabinoid receptors. *Ann N Y Acad Sci* 1139:450–457. [PubMed: 18991892]
- Burstein SR, Williams TJ, Lane DA, Knudsen MG, Pickel VM, McEwen BS, Waters EM, Milner TA (2013) The influences of reproductive status and acute stress on the levels of phosphorylated delta opioid receptor immunoreactivity in rat hippocampus. *Brain Res* 1518:71–81. [PubMed: 23583481]
- Butelman ER, Marenmani AGI, Bacciardi S, Chen CY, Correa da Rosa J, Kreek MJ (2018a) Non-medical Cannabis Self-Exposure as a Dimensional Predictor of Opioid Dependence Diagnosis: A Propensity Score Matched Analysis. *Frontiers in psychiatry* 9.
- Butelman ER, Chen CY, Fry RS, Kimani R, Levran O, Ott J, Correa da Rosa J, Kreek MJ (2018b) Re-evaluation of the KMSK scales, rapid dimensional measures of self-exposure to specific drugs: Gender-specific features. *Drug Alcohol Depend* 190:179–187. [PubMed: 30041093]
- Celio MR (1990) Calbindin D-28k and parvalbumin in the rat nervous system. *Neuroscience* 35:375–475. [PubMed: 2199841]
- Celio MR, Baier W, Schärer L, de Viragh PA, Gerday C (1988) Monoclonal antibodies directed against the calcium binding protein parvalbumin. *Cell calcium* 9:81–86. [PubMed: 3383226]
- Centers for Disease Control and Prevention (2019) Opioid overdose: Opioid data analysis and resources. In.
- Chu J, Zheng H, Loh HH, Law PY (2008) Morphine-induced mu-opioid receptor rapid desensitization is independent of receptor phosphorylation and beta-arrestins. *Cellular signalling* 20:1616–1624. [PubMed: 18558479]
- Cooper ZD, Haney M (2009) Actions of delta-9-tetrahydrocannabinol in cannabis: relation to use, abuse, dependence. *Int Rev Psychiatry* 21:104–112. [PubMed: 19367504]
- Cooper ZD, Craft RM (2018) Sex-Dependent Effects of Cannabis and Cannabinoids: A Translational Perspective. *Neuropsychopharmacology* 43:34–51. [PubMed: 28811670]

- Craft RM, Britch SC, Buzitis NW, Clowers BH (2019) Age-related differences in Delta(9)-tetrahydrocannabinol-induced antinociception in female and male rats. *Exp Clin Psychopharmacol* 27:338–347. [PubMed: 31120286]
- Crain BJ, Chang KJ, McNamara JO (1986) Quantitative autoradiographic analysis of mu and delta opioid binding sites in the rat hippocampal formation. *J Comp Neurol* 246:170–180. [PubMed: 3007584]
- Dang VC, Christie MJ (2012) Mechanisms of rapid opioid receptor desensitization, resensitization and tolerance in brain neurons. *Br J Pharmacol* 165:1704–1716. [PubMed: 21564086]
- de Miguel R, Romero J, Muñoz RM, García-Gil L, González S, Villanua MA, Makriyannis A, Ramos JA, Fernández-Ruiz JJ (1998) Effects of cannabinoids on prolactin and gonadotrophin secretion: involvement of changes in hypothalamic gamma-aminobutyric acid (GABA) inputs. *Biochem Pharmacol* 56:1331–1338. [PubMed: 9825732]
- Deutsch-Feldman M, Picetti R, Seip-Cammack K, Zhou Y, Kreek MJ (2015) Effects of handling and vehicle injections on adrenocorticotrophic and corticosterone concentrations in Sprague-Dawley compared with Lewis rats. *Journal of the American Association for Laboratory Animal Science : JAALAS* 54:35–39. [PubMed: 25651089]
- Do VH, Martinez CO, Martinez JL Jr., Derrick BE (2002) Long-term potentiation in direct perforant path projections to the hippocampal CA3 region in vivo. *J Neurophysiol* 87:669–678. [PubMed: 11826036]
- Drake CT, Milner TA (1999) Mu opioid receptors are in somatodendritic and axonal compartments of GABAergic neurons in rat hippocampal formation. *Brain Res* 849:203–215. [PubMed: 10592303]
- Drake CT, Milner TA (2006) Mu opioid receptors are extensively co-localized with parvalbumin, but not somatostatin, in the dentate gyrus. *Neurosci Lett* 403:176–180. [PubMed: 16716508]
- Drake CT, Chavkin C, Milner TA (2007) Opioid systems in the dentate gyrus. *Prog Brain Res* 163:245–263. [PubMed: 17765723]
- Ehlers CL, Gizer IR, Vieten C, Gilder DA, Stouffer GM, Lau P, Wilhelmsen KC (2010) Cannabis dependence in the San Francisco Family Study: age of onset of use, DSM-IV symptoms, withdrawal, and heritability. *Addict Behav* 35:102–110. [PubMed: 19818563]
- Elliott-Hunt CR, Kazlauskaitė J, Wilde GJC, Grammatopoulos DK, Hillhouse EW (2002) Potential signalling pathways underlying corticotrophin-releasing hormone-mediated neuroprotection from excitotoxicity in rat hippocampus. *Journal of Neurochemistry* 80:416–425. [PubMed: 11908464]
- Fernandez-Monreal M, Brown TC, Royo M, Esteban JA (2012) The balance between receptor recycling and trafficking toward lysosomes determines synaptic strength during long-term depression. *J Neurosci* 32:13200–13205. [PubMed: 22993436]
- Gonzales KL, Chappelle JD, Pierce JP, Kelter DT, Williams TJ, Torres-Reveron A, McEwen BS, Waters EM, Milner TA (2011) The influences of reproductive status and acute stress on the levels of phosphorylated mu opioid receptor immunoreactivity in rat hippocampus. *Frontiers in endocrinology* 2.
- Gulya K, Gehlert DR, Wamsley JK, Mosberg H, Hruby VJ, Yamamura HI (1986) Light microscopic autoradiographic localization of delta opioid receptors in the rat brain using a highly selective bis-benpenicillamine cyclic enkephalin analog. *J Pharmacol Exp Ther* 238:720–726. [PubMed: 3016247]
- Gulyas AI, Cravatt BF, Bracey MH, Dinh TP, Piomelli D, Boscia F, Freund TF (2004) Segregation of two endocannabinoid-hydrolyzing enzymes into pre- and postsynaptic compartments in the rat hippocampus, cerebellum and amygdala. *Eur J Neurosci* 20:441–458. [PubMed: 15233753]
- Haberstock-Debic H, Wein M, Barrot M, Colago EE, Rahman Z, Neve RL, Pickel VM, Nestler EJ, von Zastrow M, Svingos AL (2003) Morphine acutely regulates opioid receptor trafficking selectively in dendrites of nucleus accumbens neurons. *J Neurosci* 23:4324–4332. [PubMed: 12764121]
- Harte-Hargrove LC, Varga-Wesson A, Duffy AM, Milner TA, Scharfman HE (2015) Opioid receptor-dependent sex differences in synaptic plasticity in the hippocampal mossy fiber pathway of the adult rat. *J Neurosci* 35:1723–1738. [PubMed: 25632146]
- Hernandez-Avila CA, Rounsaville BJ, Kranzler HR (2004) Opioid-, cannabis- and alcohol-dependent women show more rapid progression to substance abuse treatment. *Drug Alcohol Depend* 74:265–272. [PubMed: 15194204]

- Hernández-Tristán R, Arévalo C, Canals S, Leret ML (2000) The effects of acute treatment with delta9-THC on exploratory behaviour and memory in the rat. *J Physiol Biochem* 56:17–24. [PubMed: 10879677]
- Hillhouse EW, Grammatopoulos DK (2006) The Molecular Mechanisms Underlying the Regulation of the Biological Activity of Corticotropin-Releasing Hormone Receptors: Implications for Physiology and Pathophysiology. *Endocrine Reviews* 27:260–286. [PubMed: 16484629]
- Himmel HM (2007) Suitability of commonly used excipients for electrophysiological in-vitro safety pharmacology assessment of effects on hERG potassium current and on rabbit Purkinje fiber action potential. *J Pharmacol Toxicol Methods* 56:145–158. [PubMed: 17590357]
- Hollrigel GS, Chen K, Baram TZ, Soltesz I (1998) The pro-convulsant actions of corticotropin-releasing hormone in the hippocampus of infant rats. *Neuroscience* 84:71–79. [PubMed: 9522363]
- Huestis MA, Henningfield JE, Cone EJ (1992) Blood cannabinoids. I. Absorption of THC and formation of 11-OH-THC and THCCOOH during and after smoking marijuana. *J Anal Toxicol* 16:276–282. [PubMed: 1338215]
- Johnson MA, Contoreggi NH, Kogan JF, Bryson M, Rubin BR, Gray JD, Kreek MJ, McEwen BS, Milner TA (2020) Chronic stress differentially alters mRNA expression of opioid peptides and receptors in the dorsal hippocampus of female and male rats. *Journal of Comparative Neurology*.
- Karson MA, Tang A, Milner TA, Alger BE (2009) Synaptic cross-talk between perisomatic-targeting interneuron classes expressing cholecystokinin and parvalbumin in hippocampus. *J Neurosci* 29:4140–4154. [PubMed: 19339609]
- Kawamura Y, Fukaya M, Maejima T, Yoshida T, Miura E, Watanabe M, Ohno-Shosaku T, Kano M (2006) The CB1 cannabinoid receptor Is the major cannabinoid receptor at excitatory presynaptic sites in the hippocampus and cerebellum. *J Neurosci* 26:2991–3001. [PubMed: 16540577]
- Kesner RP, Warthen DK (2010) Implications of CA3 NMDA and opiate receptors for spatial pattern completion in rats. *Hippocampus* 20:550–557. [PubMed: 19650123]
- Kieffer BL, Befort K, Gaveriaux-Ruff C, Hirth CG (1992) The delta-opioid receptor: isolation of a cDNA by expression cloning and pharmacological characterization. *Proc Natl Acad Sci U S A* 89:12048–12052. [PubMed: 1334555]
- Koob GF, Volkow ND (2010) Neurocircuitry of addiction. *Neuropsychopharmacology* 35:217–238. [PubMed: 19710631]
- Koob GF, Volkow ND (2016) Neurobiology of addiction: a neurocircuitry analysis. *The lancet Psychiatry* 3:760–773. [PubMed: 27475769]
- Lauder JM, Han VKM, Henderson P, Verdoorn T, Towle AC (1986) Prenatal ontogeny of the gabaergic system in the rat brain: An immunocytochemical study. *Neuroscience* 19:465–493. [PubMed: 3022187]
- London M, Häusser M (2005) Dendritic computation. *Annu Rev Neurosci* 28:503–532. [PubMed: 16033324]
- Luo AH, Tahsili-Fahadan P, Wise RA, Lupica CR, Aston-Jones G (2011) Linking context with reward: a functional circuit from hippocampal CA3 to ventral tegmental area. *Science* 333:353–357. [PubMed: 21764750]
- Mansour A, Khachaturian H, Lewis ME, Akil H, Watson SJ (1987) Autoradiographic differentiation of mu, delta, and kappa opioid receptors in the rat forebrain and midbrain. *J Neurosci* 7:2445–2464. [PubMed: 3039080]
- Mansour A, Fox CA, Burke S, Meng F, Thompson RC, Akil H, Watson SJ (1994) Mu, delta, and kappa opioid receptor mRNA expression in the rat CNS: an in situ hybridization study. *J Comp Neurol* 350:412–438. [PubMed: 7884049]
- Manzanedo C, Aguilar MA, Rodriguez-Arias M, Navarro M, Minarro J (2004) Cannabinoid agonist-induced sensitisation to morphine place preference in mice. *Neuroreport* 15:1373–1377. [PubMed: 15167569]
- Marques-Lopes J, Van Kempen T, Waters EM, Pickel VM, Iadecola C, Milner TA (2014) Slow-pressor angiotensin II hypertension and concomitant dendritic NMDA receptor trafficking in estrogen receptor beta-containing neurons of the mouse hypothalamic paraventricular nucleus are sex and age dependent. *J Comp Neurol* 522:3075–3090. [PubMed: 24639345]

- Marsicano G, Lutz B (1999) Expression of the cannabinoid receptor CB1 in distinct neuronal subpopulations in the adult mouse forebrain. *Eur J Neurosci* 11:4213–4225. [PubMed: 10594647]
- Mazid S, Hall BS, Odell SC, Stafford K, Dyer AD, Van Kempen TA, Selegean J, McEwen BS, Waters EM, Milner TA (2016) Sex differences in subcellular distribution of delta opioid receptors in the rat hippocampus in response to acute and chronic stress. *Neurobiology of Stress* 5:37–53. [PubMed: 27981195]
- McAlinn HR, Reich B, Contoreggi NH, Kamakura RP, Dyer AG, McEwen BS, Waters EM, Milner TA (2018) Sex differences in the subcellular distribution of corticotropin-releasing factor receptor 1 in the rat hippocampus following chronic immobilization stress. *Neuroscience* 383:98–113. [PubMed: 29753863]
- McEwen BS, Milner TA (2017) Understanding the broad influence of sex hormones and sex differences in the brain. *J Neurosci Res* 95:24–39. [PubMed: 27870427]
- McLean S, Rothman RB, Jacobson AE, Rice KC, Herkenham M (1987) Distribution of opiate receptor subtypes and enkephalin and dynorphin immunoreactivity in the hippocampus of squirrel, guinea pig, rat, and hamster. *J Comp Neurol* 255:497–510. [PubMed: 2880880]
- Mechoulam R, Parker LA (2013) The endocannabinoid system and the brain. *Annu Rev Psychol* 64:21–47. [PubMed: 22804774]
- Meilandt WJ, Barea-Rodriguez E, Harvey SA, Martinez JL Jr. (2004) Role of hippocampal CA3 mu-opioid receptors in spatial learning and memory. *J Neurosci* 24:2953–2962. [PubMed: 15044534]
- Milner TA, Pickel VM, Reis DJ (1989) Ultrastructural basis for interactions between central opioids and catecholamines. I. Rostral ventrolateral medulla. *J Neurosci* 9:2114–2130. [PubMed: 2566665]
- Milner TA, Waters EM, Robinson DC, Pierce JP (2011) Degenerating processes identified by electron microscopic immunocytochemical methods. *Methods Mol Biol* 793:23–59. [PubMed: 21913092]
- Milner TA, Burstein SR, Marrone GF, Khalid S, Gonzalez AD, Williams TJ, Schierberl KC, Torres-Reveron A, Gonzales KL, McEwen BS, Waters EM (2013) Stress differentially alters mu opioid receptor density and trafficking in parvalbumin-containing interneurons in the female and male rat hippocampus. *Synapse* 67:757–772. [PubMed: 23720407]
- Milner TA, Waters EM, Robinson DC, Pierce JP (2011) Degenerating processes identified by electron microscopic immunocytochemical methods. *Neurodegeneration, Methods and Protocols*:23–59.
- Morozov YM, Ben-Ari Y, Freund TF (2004) The spatial and temporal pattern of fatty acid amide hydrolase expression in rat hippocampus during postnatal development. *Eur J Neurosci* 20:459–466. [PubMed: 15233754]
- Nair AB, Jacob S (2016) A simple practice guide for dose conversion between animals and human. *J Basic Clin Pharm* 7:27–31. [PubMed: 27057123]
- Narimatsu S, Watanabe K, Yamamoto I, Yoshimura H (1991) Sex difference in the oxidative metabolism of 9-tetrahydrocannabinol in the rat. *Biochemical Pharmacology* 41:1187–1194. [PubMed: 1848985]
- Narimatsu S, Watanabe K, Matsunaga T, Yamamoto I, Imaoka S, Funae Y, Yoshimura H (1990) Cytochrome P-450 isozymes in metabolic activation of delta 9-tetrahydrocannabinol by rat liver microsomes. *Drug Metab Dispos* 18:943–948. [PubMed: 1981541]
- Narimatsu S, Watanabe K, Matsunaga T, Yamamoto I, Imaoka S, Funae Y, Yoshimura H (1992) Cytochrome P-450 isozymes involved in the oxidative metabolism of delta 9-tetrahydrocannabinol by liver microsomes of adult female rats. *Drug Metab Dispos* 20:79–83. [PubMed: 1347001]
- Nyiri G, Cserep C, Szabadits E, Mackie K, Freund TF (2005) CB1 cannabinoid receptors are enriched in the perisynaptic annulus and on preterminal segments of hippocampal GABAergic axons. *Neuroscience* 136:811–822. [PubMed: 16344153]
- Olive MF, Anton B, Micevych P, Evans CJ, Maidment NT (1997) Presynaptic versus postsynaptic localization of mu and delta opioid receptors in dorsal and ventral striatopallidal pathways. *J Neurosci* 17:7471–7479. [PubMed: 9295393]
- Parini P, Angelin B, Stavreus-Evers A, Freyschuss B, Eriksson H, Rudling M (2000) Biphasic effects of the natural estrogen 17beta-estradiol on hepatic cholesterol metabolism in intact female rats. *Arterioscler Thromb Vasc Biol* 20:1817–1823. [PubMed: 10894823]

- Persson AI, Thorlin T, Eriksson PS (2005) Comparison of immunoblotted delta opioid receptor proteins expressed in the adult rat brain and their regulation by growth hormone. *Neuroscience research* 52:1–9. [PubMed: 15811547]
- Pestel S, Martin HJ, Maier GM, Guth B (2006) Effect of commonly used vehicles on gastrointestinal, renal, and liver function in rats. *J Pharmacol Toxicol Methods* 54:200–214. [PubMed: 16567111]
- Peters A, Palay S, Webster H (1991) *The fine structure of the nervous system*. New York: Oxford UP.
- Pickel VM, Bourie F, Chan J, Mackie K, Lane DA, Wang G (2020) Chronic adolescent exposure to 9-tetrahydrocannabinol decreases NMDA current and extrasynaptic plasmalemmal density of NMDA GluN1 subunits in the prelimbic cortex of adult male mice. *Neuropsychopharmacology* 45:374–383. [PubMed: 31323660]
- Pierce JP, Kurucz OS, Milner TA (1999) Morphometry of a peptidergic transmitter system: Dynorphin B-like immunoreactivity in the rat hippocampal mossy fiber pathway before and after seizures. *Hippocampus* 9:255–276. [PubMed: 10401641]
- Pierce JP, Kelter DT, McEwen BS, Waters EM, Milner TA (2014) Hippocampal mossy fiber leu-enkephalin immunoreactivity in female rats is significantly altered following both acute and chronic stress. *J Chem Neuroanat* 55:9–17. [PubMed: 24275289]
- Pierce JP, Kievits J, Graustein B, Speth RC, Iadecola C, Milner TA (2009) Sex differences in the subcellular distribution of AT(1) receptors and nadph oxidase subunits in the dendrites of C1 neurons in the rat rostral ventrolateral medulla. *Neuroscience* 163:329–338. [PubMed: 19501631]
- Pradhan AA, Becker JA, Scherrer G, Tryoen-Toth P, Filliol D, Matifas A, Massotte D, Gaveriaux-Ruff C, Kieffer BL (2009) In vivo delta opioid receptor internalization controls behavioral effects of agonists. *PLoS One* 4:e5425. [PubMed: 19412545]
- Quock RM, Burkey TH, Varga E, Hosohata Y, Hosohata K, Cowell SM, Slate CA, Ehlert FJ, Roeske WR, Yamamura HI (1999) The  $\delta$ -Opioid Receptor: Molecular Pharmacology, Signal Transduction, and the Determination of Drug Efficacy. *Pharmacological Reviews* 51:503–532. [PubMed: 10471416]
- Randesi M, Zhou Y, Mazid S, Odell SC, Gray JD, Correa da Rosa J, McEwen BS, Milner TA, Kreek MJ (2018) Sex differences after chronic stress in the expression of opioid- and neuroplasticity-related genes in the rat hippocampus. *Neurobiology of Stress* 8:33–41. [PubMed: 29888302]
- Randesi M, Contoreggi NH, Zhou Y, Reich B, Bellamy JR, Yu F, Gray JD, McEwen BS, Milner TA, Kreek MJ (2019) Sex Differences in Neuroplasticity- and Stress-Related Gene Expression and Protein Levels in the Rat Hippocampus Following Oxycodone Conditioned Place Preference. *Neuroscience*.
- Reich B, Zhou Y, Goldstein E, Srivats SS, Contoreggi NH, Kogan JF, McEwen BS, Kreek MJ, Milner TA, Gray JD (2019) Chronic immobilization stress primes the hippocampal opioid system for oxycodone-associated learning in female but not male rats. *Synapse*:e22088. [PubMed: 30632204]
- Rogers SA, Kempen TA, Pickel VM, Milner TA (2016) Enkephalin levels and the number of neuropeptide Y-containing interneurons in the hippocampus are decreased in female cannabinoid-receptor 1 knock-out mice. *Neurosci Lett* 620:97–103. [PubMed: 27012427]
- Ruiz CM, Torrens A, Castillo E, Perrone CR, Cevallos J, Inshishian VC, Harder EV, Justeson DN, Huestis MA, Swarup V, Piomelli D, Mahler SV (2020) Pharmacokinetic, behavioral, and brain activity effects of Delta(9)-tetrahydrocannabinol in adolescent male and female rats. *Neuropsychopharmacology*.
- Ryan JD, Zhou Y, Contoreggi NH, Bshesh FK, Gray JD, Kogan JF, Ben KT, McEwen BS, Jeanne Kreek M, Milner TA (2018) Sex differences in the rat hippocampal opioid system after oxycodone conditioned place preference. *Neuroscience* 393:236–257. [PubMed: 30316908]
- Saland LC, Hastings CM, Abeyta A, Chavez JB (2005) Chronic ethanol modulates delta and mu-opioid receptor expression in rat CNS: immunohistochemical analysis with quantitative confocal microscopy. *Neurosci Lett* 381:163–168. [PubMed: 15882810]
- Scharfman HE, MacLusky NJ (2017) Sex differences in hippocampal area CA3 pyramidal cells. *J Neurosci Res* 95:563–575. [PubMed: 27870399]
- Schepis TS, Desai RA, Cavallo DA, Smith AE, McFetridge A, Liss TB, Potenza MN, Krishnan-Sarin S (2011) Gender differences in adolescent marijuana use and associated psychosocial characteristics. *J Addict Med* 5:65–73. [PubMed: 21769049]



- Schulz S, Mayer D, Pfeiffer M, Stumm R, Koch T, Hollt V (2004) Morphine induces terminal micro-opioid receptor desensitization by sustained phosphorylation of serine-375. *The EMBO journal* 23:3282–3289. [PubMed: 15272312]
- Sjöström PJ, Rancz EA, Roth A, Häusser M (2008) Dendritic excitability and synaptic plasticity. *Physiol Rev* 88:769–840. [PubMed: 18391179]
- Solinas M, Panlilio LV, Tanda G, Makriyannis A, Matthews SA, Goldberg SR (2005) Cannabinoid agonists but not inhibitors of endogenous cannabinoid transport or metabolism enhance the reinforcing efficacy of heroin in rats. *Neuropsychopharmacology* 30:2046–2057. [PubMed: 15870833]
- Spruston N (2008) Pyramidal neurons: dendritic structure and synaptic integration. *Nat Rev Neurosci* 9:206–221. [PubMed: 18270515]
- Swanson LW (1992) *Brain Maps: Structure of the Rat Brain*, 1 Edition. Amsterdam: Elsevier.
- Torres-Reveron A, Khalid S, Williams TJ, Waters EM, Drake CT, McEwen BS, Milner TA (2008) Ovarian steroids modulate leu-enkephalin levels and target leu-enkephalinergic profiles in the female hippocampal mossy fiber pathway. *Brain Res* 1232:70–84. [PubMed: 18691558]
- Torres-Reveron A, Williams TJ, Chapleau JD, Waters EM, McEwen BS, Drake CT, Milner TA (2009) Ovarian steroids alter mu opioid receptor trafficking in hippocampal parvalbumin GABAergic interneurons. *Exp Neurol* 219:319–327. [PubMed: 19505458]
- Tseng AH, Harding JW, Craft RM (2004) Pharmacokinetic factors in sex differences in Delta 9-tetrahydrocannabinol-induced behavioral effects in rats. *Behav Brain Res* 154:77–83. [PubMed: 15302113]
- Tsou K, Mackie K, Sanudo-Pena MC, Walker JM (1999) Cannabinoid CB1 receptors are localized primarily on cholecystokinin-containing GABAergic interneurons in the rat hippocampal formation. *Neuroscience* 93:969–975. [PubMed: 10473261]
- Turner CD, Bagnara JT (1971) *General Endocrinology*. Philadelphia: W.B. Saunders.
- Vorel SR, Liu X, Hayes RJ, Spector JA, Gardner EL (2001) Relapse to cocaine-seeking after hippocampal theta burst stimulation. *Science* 292:1175–1178. [PubMed: 11349151]
- Wiley JL, Burston JJ (2014) Sex differences in Delta(9)-tetrahydrocannabinol metabolism and in vivo pharmacology following acute and repeated dosing in adolescent rats. *Neurosci Lett* 576:51–55. [PubMed: 24909619]
- Wiley JL, Barrus DG, Farquhar CE, Lefever TW, Gamage TF (2021) Sex, species and age: Effects of rodent demographics on the pharmacology of (9)-tetrahydrocannabinol. *Prog Neuropsychopharmacol Biol Psychiatry* 106:110064. [PubMed: 32810571]
- Williams TJ, Torres-Reveron A, Chapleau JD, Milner TA (2011a) Hormonal regulation of delta opioid receptor immunoreactivity in interneurons and pyramidal cells in the rat hippocampus. *Neurobiol Learn Mem* 95:206–220. [PubMed: 21224009]
- Williams TJ, Akama KT, Knudsen MG, McEwen BS, Milner TA (2011b) Ovarian hormones influence corticotropin releasing factor receptor colocalization with delta opioid receptors in CA1 pyramidal cell dendrites. *Exp Neurol* 230:186–196. [PubMed: 21549703]
- Woodburn K, Kessel D (1994) The alteration of plasma lipoproteins by cremophor EL. *J Photochem Photobiol B* 22:197–201. [PubMed: 8014752]
- Znamensky V, Akama KT, McEwen BS, Milner TA (2003) Estrogen Levels Regulate the Subcellular Distribution of Phosphorylated Akt in Hippocampal CA1 Dendrites. *The Journal of Neuroscience* 23:2340–2347. [PubMed: 12657693]

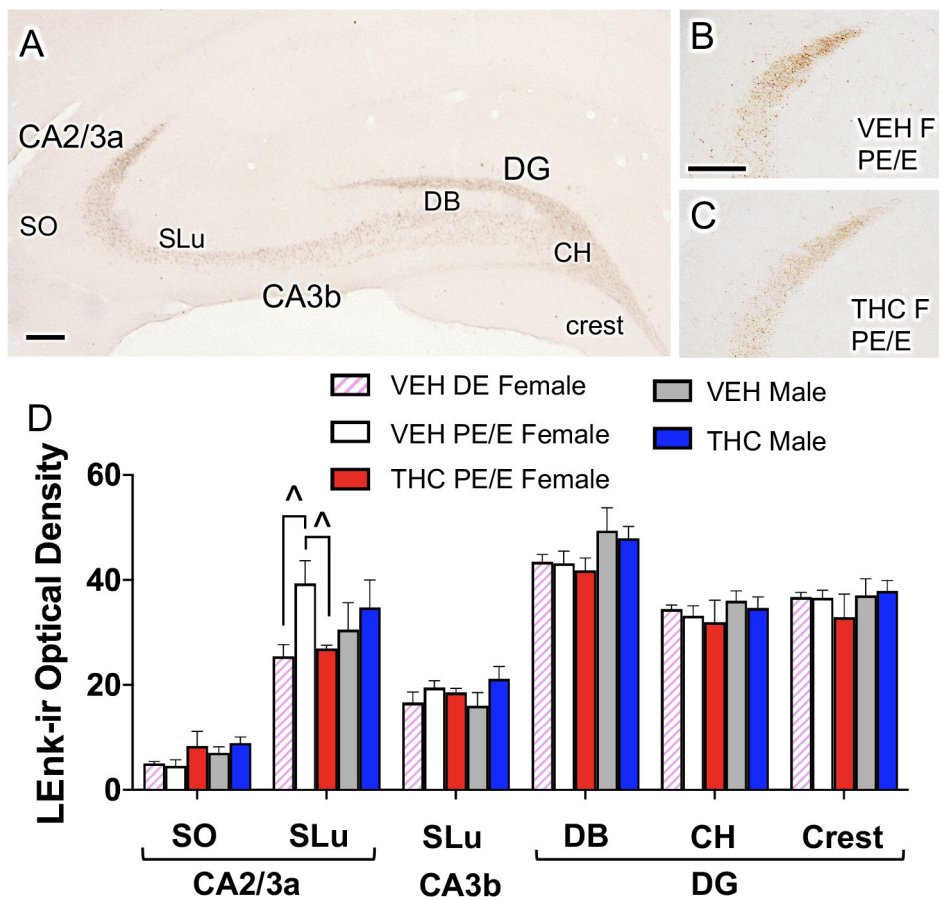


**Fig. 1.** Acute THC reduces mossy fiber Leu-Enkephalin (LEnk) levels in CA2/3a in proestrus/estrus (PE/E) female rats.

**A.** Representative light micrograph showing the regions of the CA3 and dentate gyrus (DG) from which optical density of LEnk-ir were measured. CH, central hilus; DB, dorsal blade of the hilus; SLu, Stratum lucidum; SO, stratum oriens. **B, C.** Representative micrographs show that THC PE/E females compared to VEH PE/E females have decreased LEnk labeling in the CA3a. **D.** In CA2/3a, VEH PE/E females have higher LEnk labeling compared to diestrus VEH-females. However, THC PE/E females have similar densities of LEnk in CA2/3a compared to VEH diestrus (DE) females.  $\wedge = p < 0.08$ . Scale bar = 100 microns.

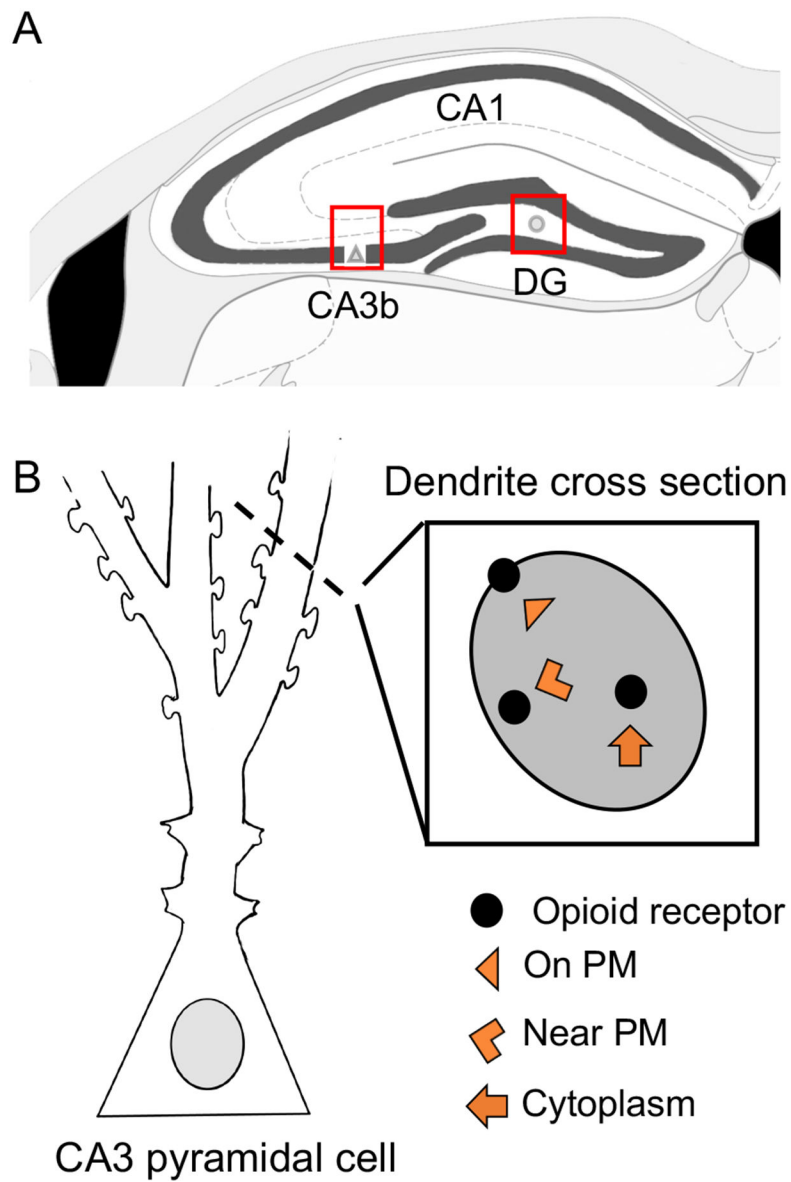


**Fig 2. Schematic of electron microscopic (EM) analysis in hippocampus.**  
**A.** DOR-labeling was analyzed in pyramidal cells in CA3b and MOR-PARV labeling was analyzed in the hilus of the dentate gyrus (DG) (boxed regions). **B.** CA3 pyramidal cell schematic and cross-section of dendrite represents the subcellular compartmentalization of the SIG-particles. PM, plasma membrane.

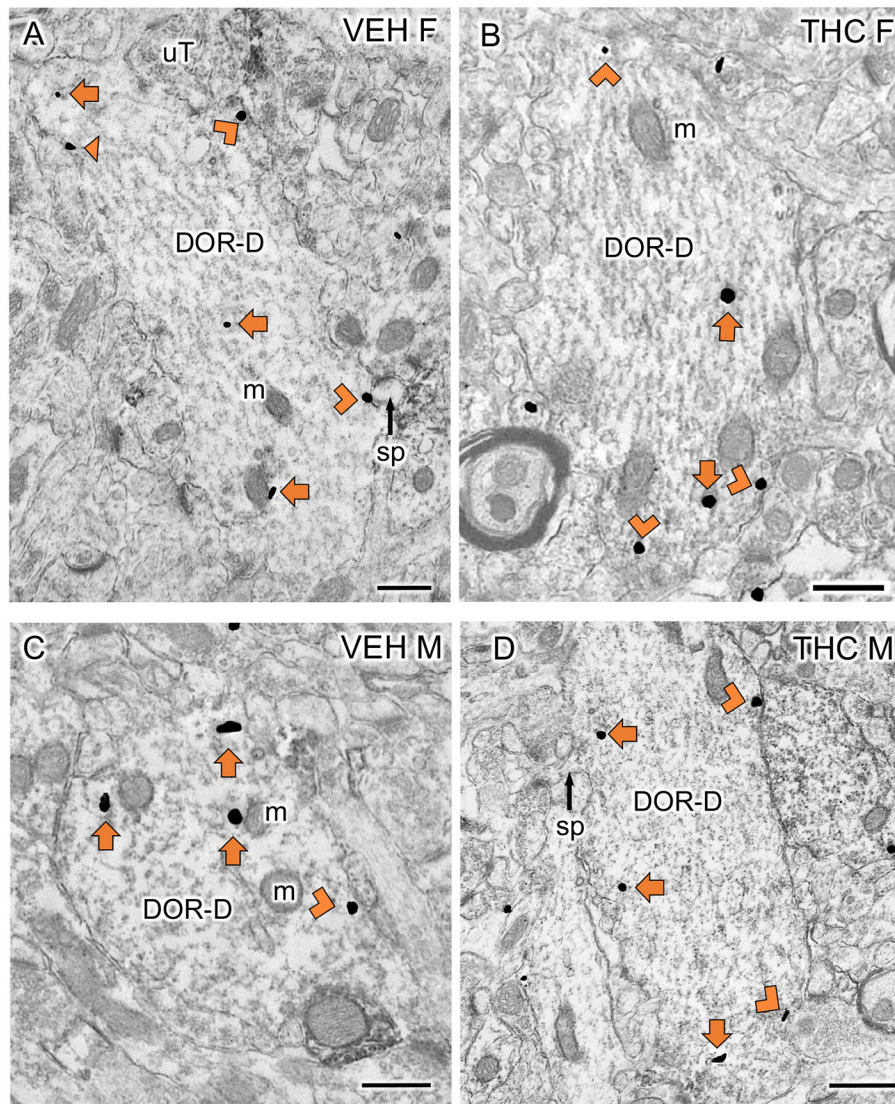


**Fig 3: Examples of delta opioid receptor (DOR)-labeled CA3 dendrites particles from VEH and THC rats.**

**A-D.** Representative EMs of DOR-labeled dendrites (DOR-D) from a VEH-female (A), THC-female (B), VEH-male (C) and THC-male (D) rat. m, mitochondria; sp, spine; uT, unlabeled terminal; Triangle, on plasma membrane SIG; Chevron, near plasma membrane SIG; Arrow, cytoplasmic SIG. Scale bar = 500 nm

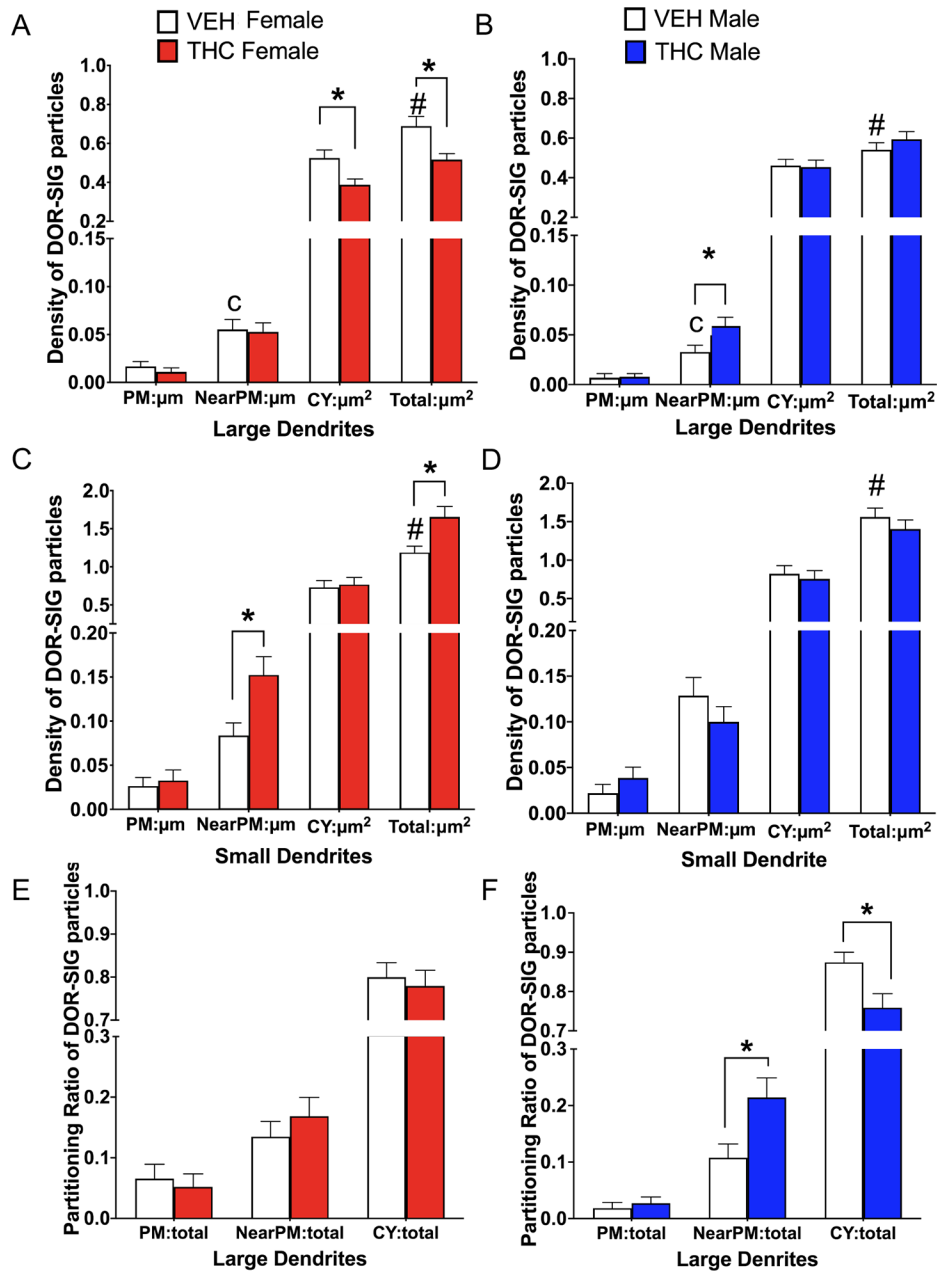


**Fig 4. Sex differences in the distribution of delta opioid receptor-silver intensified gold (DOR-SIG) within CA3 pyramidal cell dendrites in vehicle and acute THC rats.**

**A,B.** In large pyramidal cell dendrites, VEH-females tended to have more near plasma membrane DOR-SIG particles compared to VEH-males. Additionally, THC-females had reduced density of DOR-SIG particles in the cytoplasm and in total in large CA3 dendrites compared to VEH-females. THC-males had increased near plasma membrane DOR-SIG particles compared to VEH-males. **C,D.** In small pyramidal cell dendrites, VEH-females had fewer total DOR-SIG particles compared to VEH-males. THC-females had increased DOR-SIG particles near the plasmalemma and in overall total compared to VEH-females. In contrast, there were no differences in DOR-SIG density in CA3 dendrites between male

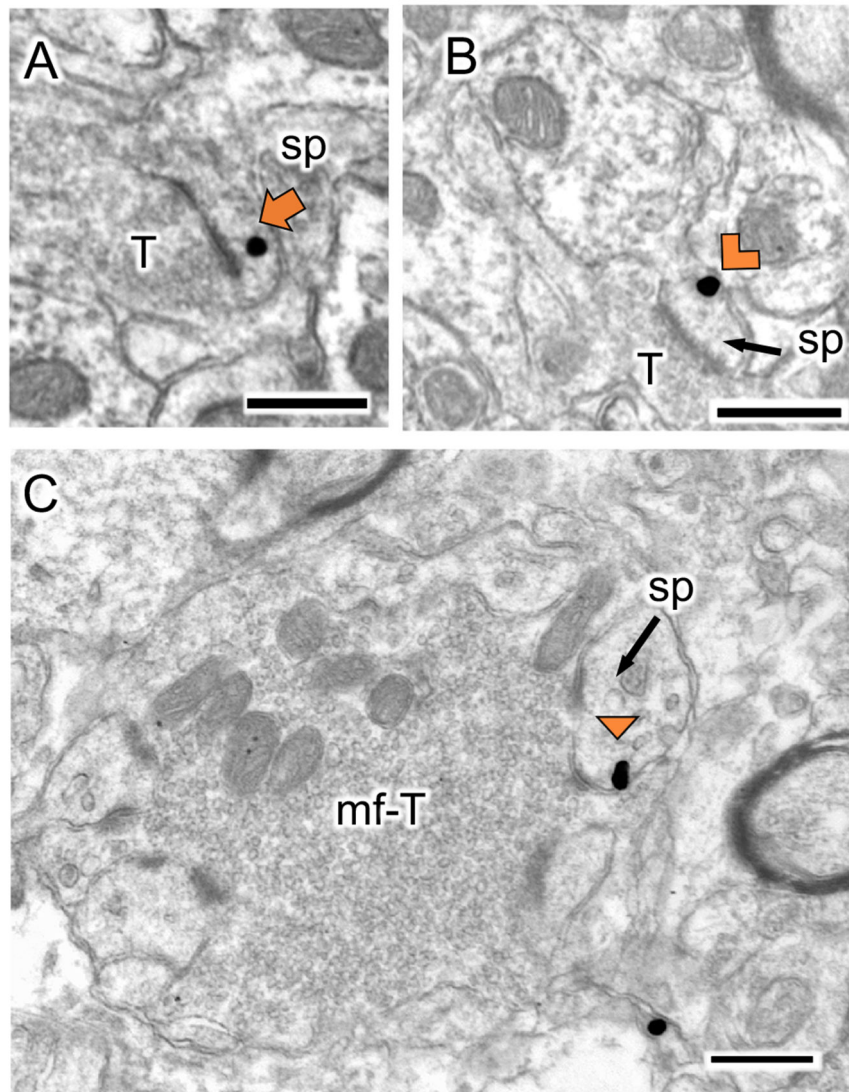
groups. **E,F**. There were no differences in the partitioning ratios of DOR-SIG particles in large CA3 dendrites in female groups. However, the partitioning ratio of DOR-SIG particles in large CA3 dendrites of THC-males compared to VEH-males increased near the plasmalemma and decreased in the cytoplasm. \* and #  $p < 0.05$ ; c =  $p = 0.08$

Author Manuscript

Author Manuscript

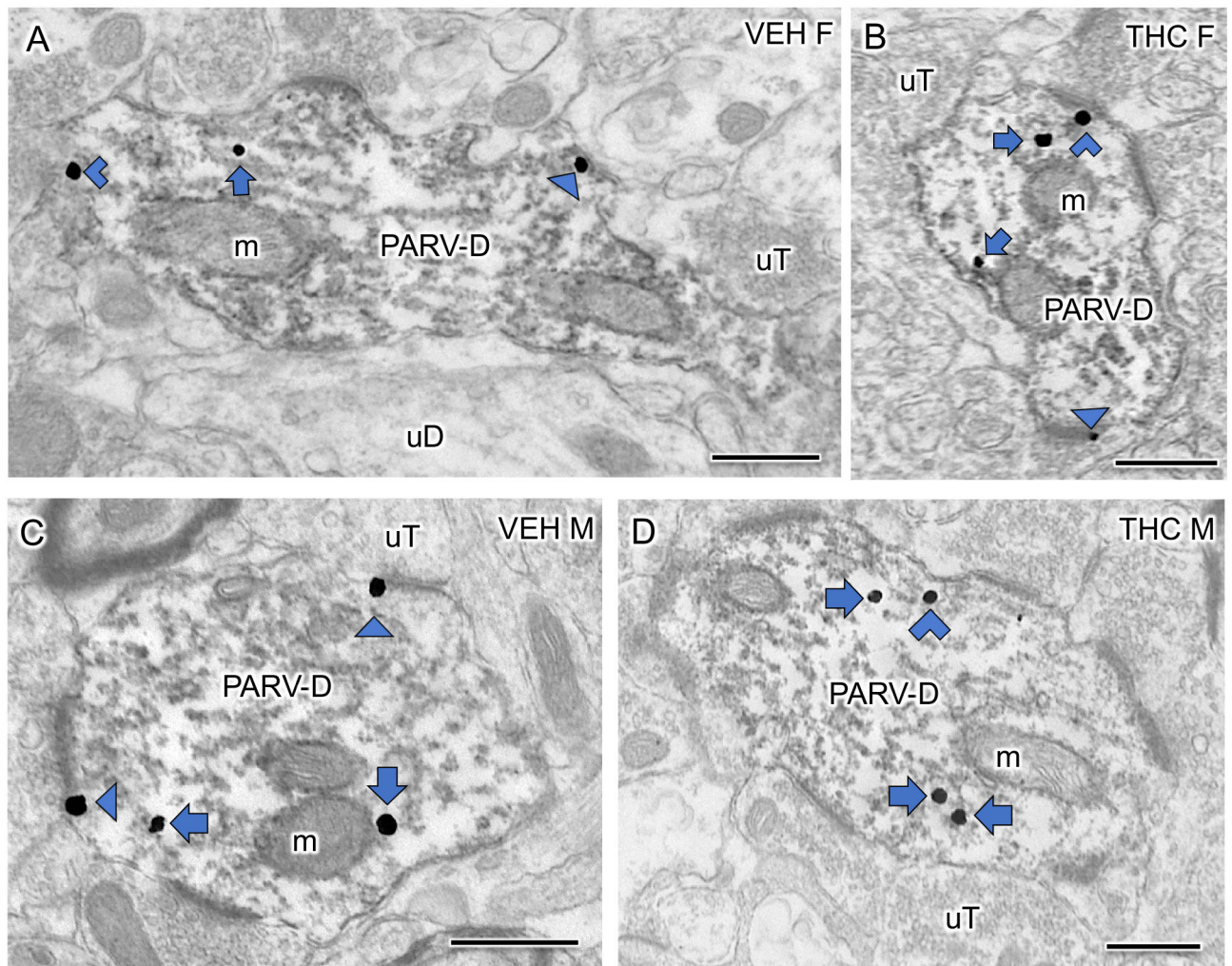
Author Manuscript

Author Manuscript



**Fig 5. Representative electron micrographs of delta opioid receptor-silver intensified gold (DOR-SIG) labeled spines in CA3.**

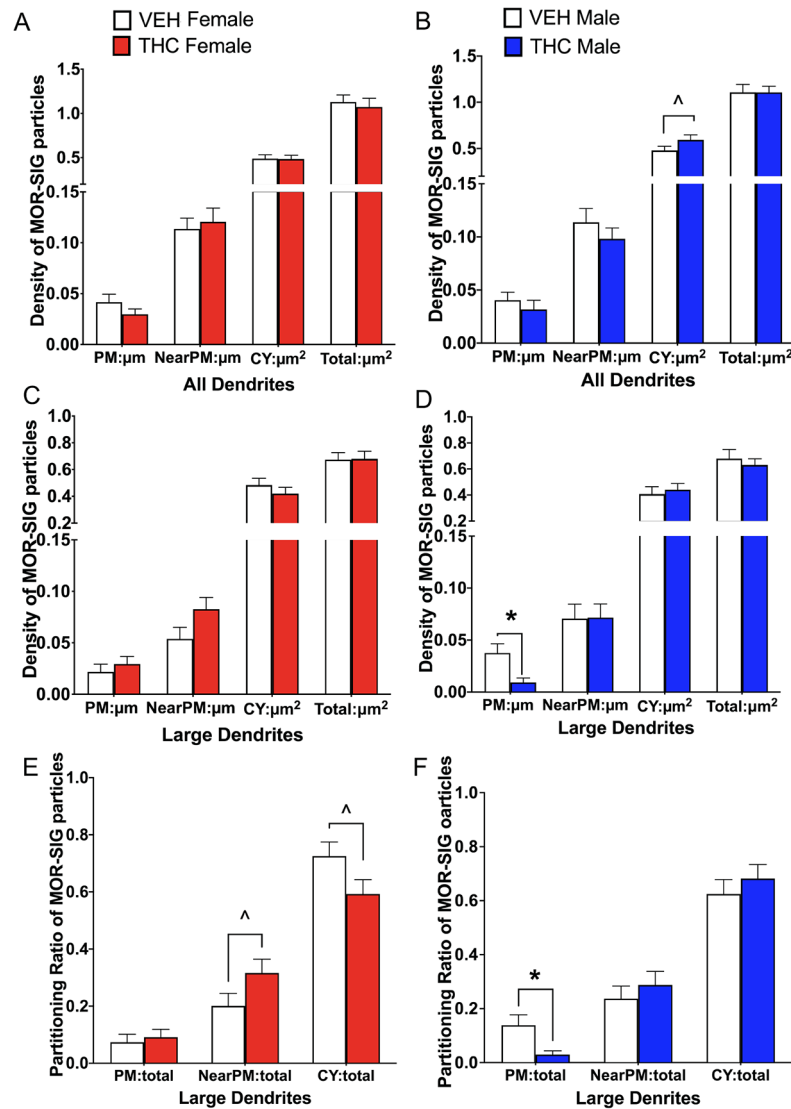
**A-B.** In SR of CA3, DOR-SIG particles are found in the cytoplasm (A) and near the plasma membrane (B). **C.** A spine with a DOR-SIG particle on the plasma membrane is contacted by mossy-fiber terminals. sp, spine; T, terminal. mf-T, mossy fiber terminal. Triangle, on plasma membrane SIG; Chevron, near plasma membrane SIG; Arrow, cytoplasmic SIG. Scale bar = 500 nm.



**Fig 6: Examples of dendrites dually labeled for mu opioid receptor (MOR) and parvalbumin (PARV) from the dentate gyrus of VEH and THC rats.**

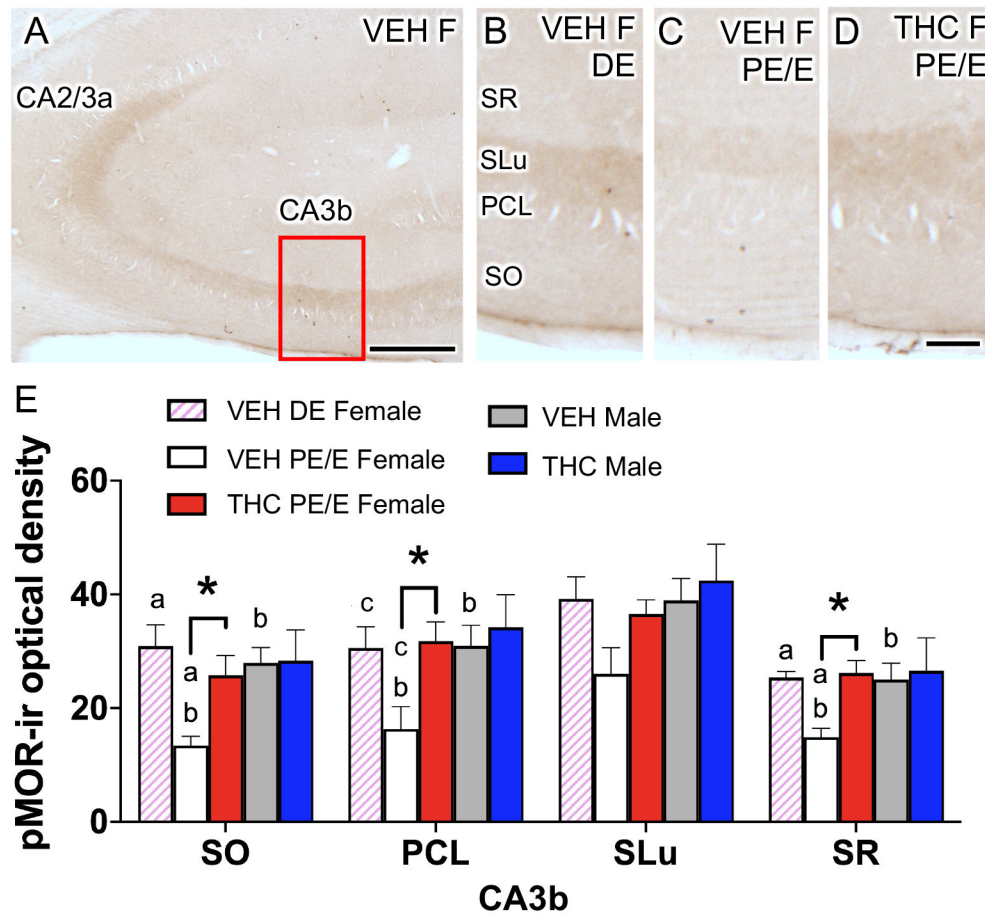
**A-D.** Representative electron micrographs of large PARV dendrites (PARV-D) dually labeled with MOR-SIG from a VEH-female (A), THC-female (B), VEH-male (C) and THC-male (D) rat. m, mitochondria; uT, unlabeled terminal; uD, unlabeled dendrite. Triangle, on plasma membrane SIG; Chevron, near plasma membrane SIG; Arrow, cytoplasmic SIG. Scale bar = 500 nm





**Fig 7. Sex differences in the distribution of mu opioid receptor silver intensified gold (MOR-SIG) particles within parvalbumin (PARV)-labeled dendrites in hilus of the dentate gyrus in VEH and THC rats.**

**A.** In female groups, there were no significant differences in the density of MOR-SIG particles in any cellular compartment of PARV dendrites. **B.** THC-males compared to VEH-males tended to have increased densities of cytoplasmic MOR-SIG particles in PARV-labeled dendrites. **C,D.** In large PARV-labeled dendrites, THC-males, but not females, had significantly less MOR-SIG particles on the plasmalemma compared to VEH-males. **E.** The partitioning ratio of MOR-SIG particles in large PARV dendrites tended to be higher near the plasmalemma and lower in the cytoplasm of THC-females compared to VEH-females. **F.** The partitioning ratio of MOR-SIG particles in large PARV dendrites was significantly less on the plasma membrane in THC-males compared to VEH-males. \*  $p < 0.05$ ; ^  $p < 0.08$ .







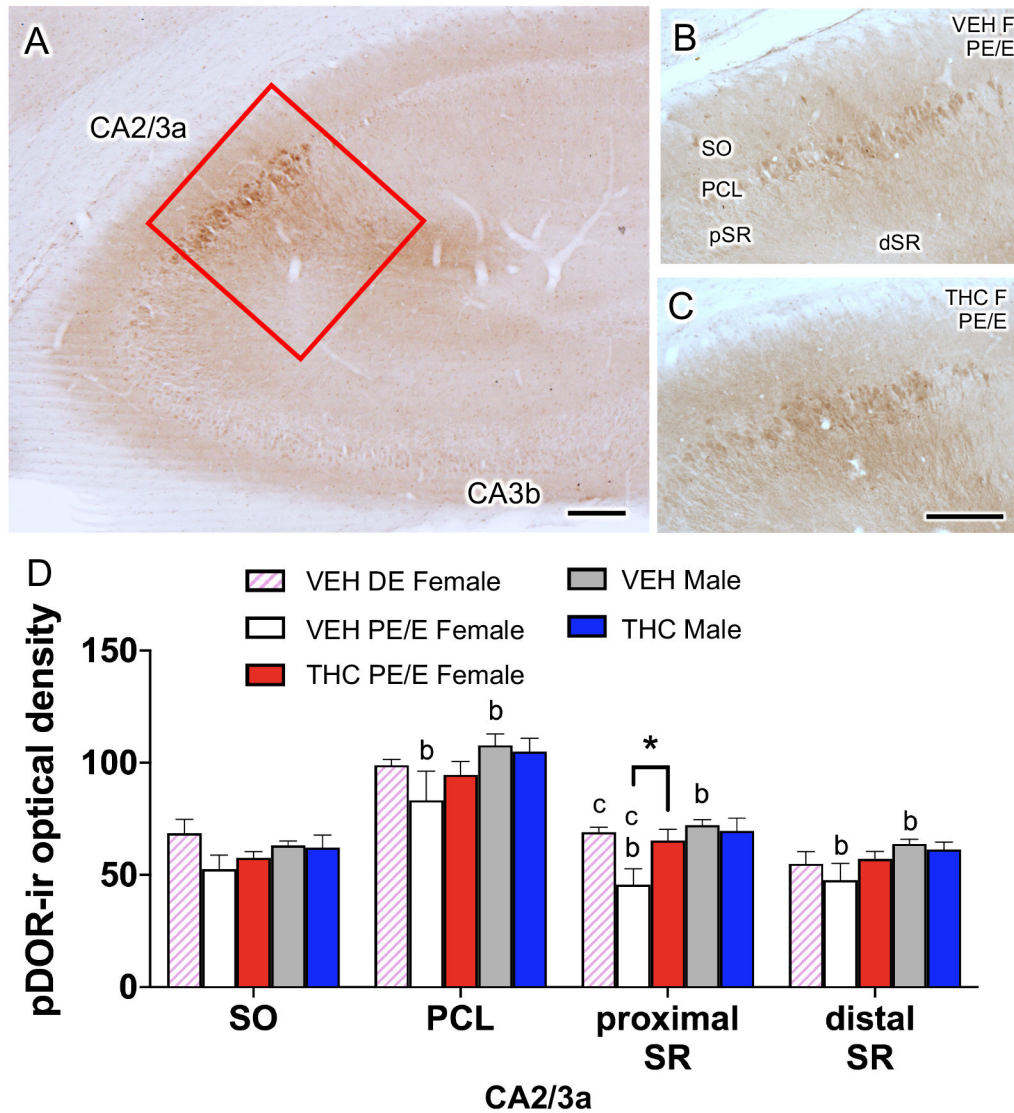











**Fig 8. Sex differences in phosphorylated mu opioid receptor (pMOR) levels within the CA3b in VEH and THC female and male rats.**

**A.** Low magnification light micrograph of pMOR-labeling shows the CA3b region of the hippocampus (box) that was sampled for analysis. **B-D.** Representative micrographs of pMOR-ir in CA3b from diestrus (DE) VEH females and proestrus/estrus (PE/E) THC females. **E.** In all laminae, except the SLu, of the CA3b, PE/E VEH females had significantly less pMOR labeling compared to PE/E THC females, DE VEH females, and VEH males. PCL, pyramidal cell layer; SLu, stratum lucidum; SO, stratum oriens; SR, stratum radiatum. \*, a and b  $p < 0.05$ ; c  $p = 0.06$ . Scale bar = 0.5 mm



**Fig 9. Sex differences in phosphorylated delta opioid receptor (pDOR) levels within the CA2/3a in VEH and THC rats.**

**A.** Low magnification light micrograph of pDOR-labeling shows the CA2/3a region of the hippocampus (box) that was sampled for analysis. **B,C.** Representative micrographs of pDOR-ir from CA2/3a from proestrus/estrus (PE/E) VEH and THC female rats. **D.** PE/E VEH-females compared to VEH-males had lower levels of pDOR-ir in the pyramidal cell layer (PCL), proximal and distal stratum radiatum (SR). pDOR-ir was significantly higher in THC-females in the proximal SR compared to VEH-females. \*, a, and b  $p < 0.05$ ; c =  $p = 0.07$ . Scale bar = 0.5 mm

Opioid marker	region	Vehicle		THC	
		Female	male	female	male
 LEnk	MF CA3a	DE < PE/E		 PE/E	
 DORs in CA3 pyramidal cell dendrites	on PM				
	near PM		M < PE/E	 PE/E (S)	 (L)
	cyto			 PE/E (L)	
	total		M < PE/E (L)	 PE/E (L)	
 pDOR	CA3a	DE > PE/E	M > PE/E	 PE/E	
 DOR spines	MF-CA3		M < PE/E		
DOR spines	CA3 SR		M < PE/E		
 MORs in PARV dendrites	on PM				 (L)
	near PM				
	cyto				
	total				
pMOR	MF CA3b	DE > PE/E	M > PE/E	 PE/E	

(L) = Large dendrites

(S) = Small dendrites

**Fig. 10. Comparison of sex differences in the rat hippocampal opioid system following VEH and acute THC injection.**

Greater than (>) or less than (<) symbols indicate baseline sex differences in VEH-injected rats. PE/E, proestrus estrus; DE, diestrus. Red arrows indicate increases whereas blue arrows indicate decreases following acute THC injections.

**Table 1**

## DOR labeled spines in CA3

Group	% ± SEM labeled spines	# ± SEM labeled spines	Location		
			Synapse	Membrane	Cytoplasm
<i>Stratum Lucidum</i>					
VEH-female	5.9 ± 2.7	6.6 ± 2.7	2	13	8
THC-female	5.9 ± 0.7	9.3 ± 1.2	3	8	17
VEH-male	9.3 ± 1.7*	12.6 ± 0.8	0	8	29
THC-male	3.0 ± 0.9*	4.0 ± 1.0	0	0	12
<i>Stratum Radiatum</i>					
VEH-female	9.0 ± 1.7 <sup>^</sup>	9.0 ± 1.7 <sup>^</sup>	5	8	14
THC-female	7.3 ± 1.2 <sup>#</sup>	7.3 ± 1.2 <sup>#</sup>	4	8	10
VEH-male	4.3 ± 0.3 <sup>^</sup>	4.3 ± 0.3 <sup>^</sup>	3	3	7
THC-male	2.6 ± 0.6 <sup>#</sup>	2.6 ± 0.6 <sup>#</sup>	0	4	4

Stratum Lucidum: All spines were counted from 50 mossy fibers.

Stratum Radiatum: 100 spines were counted from randomly selected micrographs.

Data is presented at Mean ± SEM. "Location" represents the totals from each group (N=6)

\*  
p < 0.05

<sup>^</sup>  
p = 0.07

<sup>#</sup>  
p = 0.04